

Authors are encouraged to submit new papers to INFORMS journals by means of a style file template, which includes the journal title. However, use of a template does not certify that the paper has been accepted for publication in the named journal. INFORMS journal templates are for the exclusive purpose of submitting to an INFORMS journal and should not be used to distribute the papers in print or online or to submit the papers to another publication.

The Normalization of Consumer Valuations: Context-Dependent Preferences from Neurobiological Constraints

Ryan Webb

Rotman School of Management & Department of Economics, University of Toronto, Toronto, Ontario, ryan.webb@utoronto.ca

Paul W. Glimcher

Institute for the Interdisciplinary Study of Decision-Making, New York University, 4 Washington Pl., NY, NY, 10003,
pg3@nyu.edu

Kenway Louie

Institute for the Interdisciplinary Study of Decision-Making, New York University, 4 Washington Pl., NY, NY, 10003,
kl837@nyu.edu

A long line of empirical research documents that consumer valuations are shaped by choice sets, yielding patterns of substitution between alternatives as choice sets are varied. Building on recent neuroeconomic evidence that valuations are transformed during the choice process, we incorporate the canonical *divisive normalization* computation into a discrete choice model and characterize its implications for consumer choice. We find that divisive normalization predicts choice behaviour that depends on both the size and composition of the choice set and examine evidence for such behaviour from two experiments. Divisive normalization more accurately captures observed behaviour compared to alternative models, including a *range normalization* model, and is robust across experimental paradigms. Finally, we demonstrate that divisive normalization implements an efficient means for the brain to represent valuations given neurobiological constraints, yielding the fewest choice errors possible.

1. Introduction

Consider a single bar of chocolate. In the study of consumer choice, it is typically assumed that a consumer has a valuation of this chocolate bar and that this valuation can be measured (say, by a willingness-to-pay mechanism, or a rating scale). While any number of factors might determine a consumer's valuation, like the amount, type, or "nuttness" of the chocolate, a standard assumption is that this valuation is stable; when faced with a variety of other alternative chocolate bars, the

consumer's choice should be determined by their willingness-to-pay for each item individually.¹ In this article, we study how consumer valuations might instead be shaped by the composition of the choice set during the decision-making process.

How consumer preferences depend on the elements of a choice set, and why they might differ from a strict rational benchmark, has long been of interest to behavioural science. A long literature demonstrates systematic inconsistency between independent willingness-to-pay measures and the valuations implied from choices between pairs of alternatives (Slovic and Lichtenstein 1983). This has led to a recognition that preferences are typically constructed at the time of choice, rather than simply stored, retrieved, and compared (Lichtenstein and Slovic 2006, Weber and Johnson 2009). The process by which this value information is accumulated and compared in a decision can bias preferences toward an alternative simply because of the constraints involved in simultaneously processing information about both choice alternatives (Krajbich et al. 2010, Polania et al. 2019).

Beyond binary choice, an early sufficient condition for rational choice models held that relative preferences (i.e. relative choice probabilities) between any two alternatives should be independent of all others, formally stated as the axiom of Independence of Irrelevant Alternatives (IIA; Luce 1959). This axiom served as a benchmark because, if IIA is satisfied, it is sufficient to represent a decision maker's preferences with a *random utility* and analyze their choice behaviour with the familiar Multinomial Logit model (McFadden 2001, for a review). Not surprisingly, IIA places strong conditions on behaviour (Debreu 1960) and violations have been well-documented empirically at both the population and individual level (Rieskamp et al. 2006). These violations consist of patterns of substitution between alternatives as the composition of the choice set is varied.

Some forms of IIA violations can be rationalized by placing different distributional assumptions on the random utility representation (Train 2009). This includes allowing the variance of a random utility to depend on the composition of the choice set, an issue particularly critical to analyzing consumer choice data in both the lab and field (Louviere et al. 2002, Salisbury and Feinberg 2010). This modelling approach, however, is — by definition — agnostic about the process by which decisions are made. Linking the choice model more tightly to the decision process can therefore lead to a better-performing model. In this article, we leverage recent neurobiological evidence to model how valuations are transformed and compared in the decision-making process. Similar to perceptual systems in the brain, we focus on the role of neurobiological constraints in shaping the valuations of choice alternatives according to a neural computation called *divisive normalization*.

¹ Otherwise, if valuations can arbitrarily depend on other alternatives, a sequence of choice sets and auctions can be constructed that would reveal a cycle in choice behaviour. Such cycles would violate the transitivity axiom, one of the two necessary conditions underlying a deterministic rational choice model (Samuelson 1948). In a stochastic setting, choice probabilities could violate Weak Stochastic Transitivity, which Rieskamp et al. (2006) refer to as “perhaps the weakest bound on rationality.”

We then embed divisive normalization in a discrete choice model, examine the substitution patterns which result, and compare them to both standard random utility formulations as well as other recent models proposed to incorporate bound constraints.

1.1. Neurobiological Constraints on Choice

The observation that biology influences choice behaviour is not novel (Robson 2001a, Robson and Samuelson 2010, Netzer 2009, Alonso et al. 2014). This includes the observation that a constrained decision process implies behaviour we might strictly term irrational ex-ante, but is in fact an optimal response to some constraint (Simon 1979).² Like constraints traditionally described in economics, neurobiological constraints arise from scarcity. Neurons require energy in order to transmit information, and resources must be allocated to various neural systems for various tasks. This fundamental constraint has two important implications for neural computation.

Neural activity is stochastic. Stochasticity in neural activity arises, at least in part, from the small-scale thermodynamic processes involved in the transmission of information between neurons (Mainen and Sejnowski 1995, Stevens 2003, Glimcher 2005). Increasing the number (or size) of neurons that participate in a computation can only partially mitigate this stochasticity (Shadlen and Newsome 1998) and this is costly in terms of resources. Ultimately, this stochasticity influences the discriminability of quantities encoded by neural activity, yielding a degree of stochastic behaviour (Glimcher 2005).

The brain encodes information in relative terms. The relative coding of information by neural systems is one of the fundamental observations of neuroscience in the past century (Hartline and Ratliff 1957). Because neural activity is bounded – in terms of the dynamic range of a single neuron and the finite number of neurons in a brain area – computational algorithms have evolved which efficiently compress the objective state of the world for subjective perception.³ This relative representation of information is observed to be a general feature of sensory coding (Carandini and Heeger 2012), and more recently, has been observed in the neural computations of value information (for reviews, see Seymour and McClure 2008, Rangel and Clithero 2012, Louie et al. 2015).

Our contribution is to examine *how* choice-set dependence arises in a decision process which obeys neurobiological constraints, and to formally test predictions on what form it will take. We

²The recent literature on *rational inattention*, for example, examines how constraints on information-processing (Shannon 1948) can explain observed departures from rational expectations, expected utility, and the random utility model (Sims 2003, Woodford 2012, Caplin and Dean 2015).

³On the retina, for example, light intensity is encoded relative to average ambient illumination; this process of light adaptation is why black type on white newspaper appears the same in a darkened room and under bright sunlight, even though the newsprint may reflect orders of magnitude more photons in the latter environment. We survey this literature in Appendix A.1.

consider a bounded function which is tasked with identifying the highest-valued alternative in a choice set.⁴ For guidance on the form of this function, and its role in shaping valuations during the decision process, we turn to the neurobiological evidence.

1.2. Divisive Normalization

Divisive Normalization is a pervasive computation in cortex which implements a relative coding of information (Carandini et al. 1997, Schwartz and Simoncelli 2001). Originally observed in the cortical regions of the brain involved in visual perception (Heeger 1992), divisive normalization has been documented across sensory modalities and across species ranging from invertebrates to primates (Carandini and Heeger 2012). More recently, evidence for normalization has been observed in the neural computation of valuations while subjects evaluate potential choice alternatives: neural activity associated with the value of a choice object is suppressed by the valuation and number of other alternatives (Louie et al. 2011, Holper et al. 2017). We review this empirical literature in more detail in Appendix A.2.

Divisive Normalization is a simple neural computation that can be implemented by only a few neurons in a cortical circuit; mathematically, it can be represented by a function which scales, or normalizes, its inputs (Louie et al. 2014, LoFaro et al. 2014). Consider first a simplified form of the Divisive Normalization function,

$$z_i(\mathbf{v}) = \frac{v_i}{\|\mathbf{v}\|_\beta}, \quad (1)$$

where each element of an input vector $\mathbf{v} = [v_1, \dots, v_N] \in \mathbb{R}_+^N$ is scaled by the magnitude and number of its elements by a norm of degree β , denoted $\|\mathbf{v}\|_\beta \equiv \left(\sum_{n=1}^N v_n^\beta\right)^{\frac{1}{\beta}}$. If we take the inputs v_i to represent some independent valuation of an alternative i , and $z_i(\mathbf{v})$ to represent the transformation of each alternative in a choice set at the time of decision, then each alternative is normalized with respect to the entire vector of alternatives, yielding a bounded function with a relative relationship between alternatives.⁵

To establish both the positive and normative implications of Divisive Normalization, in Section 3 we incorporate a general form of (1) directly within a discrete choice model and demonstrate how choice probabilities depend on the size and composition of the choice set. Previous work has

⁴ Robson (2001b) and Rayo and Becker (2007) first considered the properties of an optimal value function given i.) the limited perception of small differences in value, and ii.) the value function is bounded above and below. Using a metaphorical principal-agent environment to mimic evolutionary forces, they demonstrate that the optimal value function must be adaptive and depend on the distribution of alternatives in the choice set. Li et al. (2017) demonstrate this result numerically for a class of bounded functions. See also Alonso et al. (2014) for an argument for why an optimal allocation of neural resources might be bounded.

⁵ This form of normalization has been previously studied in the sensory perception literature (Lyu and Simoncelli 2008, Lyu 2011, Sinz and Bethge 2013, Ballé et al. 2016a). Its role is to remove high-order correlations from natural images (e.g. Ballé et al. 2016b). Typical implementations of normalization consider a range for β between 2 and 3 in sensory systems. See Appendix A.1 for more detail.

demonstrated that a simple form of normalization (with $\beta = 1$) is qualitatively consistent with violations of the IIA axiom (Louie et al. 2013). Here, we fully characterize the substitution patterns that arise from a general form of (1) when adding *and* altering alternatives in the choice set. We demonstrate how this general formulation can be estimated and tested formally with discrete choice data, how it incorporates some existing forms of normalization as a special case, and contrast its predictions with alternative models.

For example, Divisive Normalization predicts a decrease in the likelihood of choosing a high-valued alternative as low-valued alternatives are added or manipulated. Consider two alternatives which, when evaluated independently, have valuations $v_1 > v_2 \geq 0$. Under divisive normalization, introducing a third alternative $v_3 < v_2$ to this choice set shrinks the difference between $z_1(\mathbf{v}) - z_2(\mathbf{v})$. This gap shrinks further as the value of this third alternative increases, or as more lower-valued alternatives are added. Provided a stochastic model in which choice probabilities depend on valuation differences, normalization therefore predicts how the probability of choosing the highest-valued alternative depends on the set of alternatives. This yields novel forms of IIA violations and choice probabilities compatible with Weber scaling (Weber 1834), and imposes a precise specification for how the variance of the model differs over choice sets.

However, even in the absence of normalization, it is not immediately clear that a random utility model cannot capture such substitution patterns. While the Multinomial Logit obviously predicts no IIA violations as v_3 is altered, the flexible Multinomial Probit (MNP) formulation can capture a wide variety of substitution patterns, thus may outperform a model with Divisive Normalization. Alternative forms of normalization, such as scaling valuations by their range rather than their sum (Soltani et al. 2012, Bushong et al. 2016), also make predictions about the pattern of context-dependent choice (see Section 3.2).

To sort between these different explanations, in Section 4 we estimate and test the predictions of a general normalization model in two behavioural experiments: one previously reported trinary choice experiment which varies the composition of the choice set (Louie et al. 2013), and a second novel experiment which varies the size of the choice set. Importantly, our modelling approach nests competing accounts for IIA violations. We find strong evidence for Divisive Normalization; neither the MNP nor Range Normalization are able to capture the substitution patterns we observe. Our structural specification also provides an estimate for the degree of normalization β that is larger than the simple form (with $\beta = 1$), and we find evidence that recurrent connections are more strongly-weighted in the normalization equation than all others.

Our structural approach to model testing has one other advantage: the resulting estimates of normalization parameters can be used to examine the robustness of each model.⁶ Our second

⁶ The term “structural” is used in the econometrics literature to describe whether a model is imposed on the data for the purposes of estimating parameters that are believed to be invariant and informative, in contrast with a “reduced

experiment, conducted on a separate subject sample, therefore allows us to assess each model's performance in a strict out-of-sample prediction exercise. Notably, the estimates from the Divisive Normalization model in the trinary experiment provide a good prediction of the choice probabilities in the second experiment that varies the size of the choice set; this out-of-sample prediction performs better than both a standard Probit and a Range Normalization model fit in-sample.

From a normative standpoint, Divisive Normalization has also been shown to yield an efficient coding of sensory information in a constrained neural system (Schwartz and Simoncelli 2001, Wainwright et al. 2001, Sinz and Bethge 2013, Qamar et al. 2013). However, the normative implications for choice behaviour have remained unclear, particularly because Divisive Normalization predicts a decrease in the likelihood of choosing a higher-valued alternative as low-valued alternatives are manipulated or as the choice set is expanded (up to 20% observed for the largest choice sets in our experiment). In the absence of constraints, such behaviour can be strictly termed inefficient. However, given neurobiological constraints, Divisive Normalization implements choice behaviour that is optimal (in the sense of minimizing choice errors).⁷ We thus offer one explanation for why — on a neurobiological level — boundedly rational behaviours exist. Taken all together, these results emphasize both the positive and normative advances offered by developing choice models grounded in neuroscience.

2. Model

To highlight the role of normalization in shaping valuations during a decision, we present a simple “two-stage” model of decision-making (Glimcher 2011, Fehr and Rangel 2011, Webb et al. 2019). The distinction between these stages lies in brain regions that aggregate value information in an action-independent manner and those that employ that value information in the process of choice (Platt and Plassmann 2013, Polania et al. 2015). Here, we adopt this two-stage model to demonstrate how the Divisive Normalization computation shapes valuations in a discrete choice model. For a more nuanced discussion of the empirical literature underlying this modelling approach, see Appendix A.3.

We begin by defining a quantity called *subjective value* that carries information about the valuations of each alternative in a choice set of size N . These valuations are denoted by the vector

form” analysis which places as few modelling assumptions on the data as possible (such as examining summary statistics). In cognitive psychology, it is much more common to build and estimate “process” models (what economists might call “structural” models).

⁷ Building on prior work by Swait and Marley (2013) that relates Shannon entropy to a generalized Logit, Stevenson et al. (2018) develop a normative foundation for Divisive Normalization by optimizing the tradeoff between the cost of errors and the cost of reducing stochasticity.

$\mathbf{v} = [v_1, \dots, v_N] \in \mathbb{R}_+^N$, where v_i is the valuation of each alternative $i \in \{1, \dots, N\}$.⁸ Without loss of generality, we will assume that the first alternative has largest valuation, so $v_1 > v_j, \forall j \neq 1$. To isolate the behavioural implications of Divisive Normalization, we will assume that a particular observation of \mathbf{v} has been realized, thus it is deterministic in the subsequent analysis. In our empirical analysis, we will measure this valuation with a standard willingness-to-pay mechanism independently for each item (Becker et al. 1964).⁹

The second stage of the model involves the comparison of subjective value for the purpose of choice. This is where we will explore the implications of neurobiological constraints. In particular, we consider a function which maps the valuations of all alternatives in the choice set into a common, bounded, region of neural activity for comparison. Formally, we define $z(\mathbf{v}) : \mathbb{R}_+^N \rightarrow Z$ which maps \mathbf{v} to a vector $[z_1(\mathbf{v}), \dots, z_N(\mathbf{v})]$ in a compact subspace $Z \equiv [0, \bar{z}]^N \subset \mathbb{R}_+^N$. The bound constraint is therefore given by $0 < \bar{z} < \infty$.

In Section 2.1 we will examine the role of the divisive normalization function

$$z_i(\mathbf{v}) = \frac{v_i}{\sigma + \omega \left(\sum_n v_n^\beta \right)^{\frac{1}{\beta}}}. \quad (2)$$

in implementing the bound constraint \bar{z} . In this general formulation, the parameter σ determines how neural activity saturates with increased input and can be interpreted as the baseline activity level of neurons in the normalization pool. The weight ω determines the contribution to the normalization pool for each alternative. If $\omega = 0$, there is no normalization.

⁸ Note that this definition is general enough to incorporate a range of discrete choice models which take observable attributes as arguments. For instance, a realization of \mathbf{v} can be constructed via a behavioural theory linking different attributes \mathbf{x} to valuations, $\mathbf{v} = V(\mathbf{x})$, whether those attributes are defined either objectively as sensory input or only latently (Bhatia and Stewart 2018). We strongly suspect that the brain implements relative coding in earlier stages of the decision-making process — for instance in the construction of \mathbf{v} . The existence of some form of relative coding in attribute integration essentially follows both from the results in Rayo and Becker (2007) and the neurobiological evidence for sensory systems (see Appendix A.1). Here, we restrict our attention to the role of value normalization that has been empirically documented in parietal regions of the primate brain (see Appendix A.2). We do so to provide a parsimonious account of the role of neurobiological constraints — and normalization in particular — in predicting context-dependent choice patterns beyond the multi-attribute domain typically studied. In recent work extending normalization to the multi-attribute domain, Landry and Webb (2019) address a range of phenomena including well-known decoy effects that rely on a particular structure of numerically-presented attributes (Huber et al. 1982, Simonson 1989, Tversky 1972). The fundamental feature of this, and a number of other models in the literature, is an aggregation and transformation of attribute information into a decision variable for each alternative (e.g. Trueblood et al. 2014, Tsetos et al. 2010, Noguchi and Stewart 2018). The model of value normalization presented here cannot mimic some features of these attribute-based models. For example, if $v_1 > v_2 > v_3$ then $z_1(\mathbf{v}) > z_2(\mathbf{v})$ for all values of v_3 , therefore the ordering of alternatives can never switch (we discuss violations the Regularity axiom further in Appendix B). We believe a choice model with multiple stages of normalization is of great interest, see Zimmermann et al. (2018) for an initial example.

⁹ Neural correlates of willingness-to-pay measures in pre-frontal brain regions are described in (Plassmann et al. 2007, Chib et al. 2009).

Finally, the choice process is modelled by the decision vector $\mathbf{u} = z(\mathbf{v}) + \boldsymbol{\eta}$, which appends a stochastic term $\boldsymbol{\eta} = [\eta_1, \dots, \eta_N] \in \mathbb{R}^N$ to the normalized valuations. The decision-maker chooses option i when

$$\begin{aligned} u_i &> u_j, \quad \forall j \neq i \\ z_i(\mathbf{v}) + \eta_i &> z_j(\mathbf{v}) + \eta_j, \quad \forall j \neq i \end{aligned} \quad (3)$$

yielding a probability of choosing i ,

$$P_i(z(\mathbf{v})) = \int \mathbb{1}[z_i(\mathbf{v}) - z_j(\mathbf{v}) > \eta_j - \eta_i, \quad \forall j \neq i] f(\boldsymbol{\eta}) d\boldsymbol{\eta}, \quad (4)$$

which depends on the probability density function $f(\boldsymbol{\eta})$.¹⁰

We therefore interpret \mathbf{v} as a decision maker's independent valuation of a consumer good, and we study the choice behaviour implied when these valuations are normalized, via $z(\mathbf{v})$, in the implementation of a decision.

2.1. Implementing the Bound Constraint via Normalization

Upon initial consideration, a range of possible constraints on the allocation of neural activity are possible. Most leniently, the neural activity of each alternative could be non-rivalrous, thus any activity levels $z(\mathbf{v}) \in Z$ are feasible. This is the constraint depicted in Figure 1, where each $z_i(\mathbf{v}) \leq \bar{z}$. At the other extreme, the neural activity could be perfectly rivalrous, resulting in the linear constraint $\sum_i z_i(\mathbf{v}) \leq \bar{z}$. Of course, a non-linear constraint can lie between these two extremes.

The critical feature of the Divisive Normalization is that it scales neural activity to the boundary of these possible constraints, depending on the form of the normalization. For exposition, we present these results for the simple form of normalization given in Equation (2) with $\sigma = 0$. In our empirical results in Section 4, we will consider more general forms. Appendix ?? explores the implications of relaxing this assumption on σ in more detail.

We begin with the linear constraint. If $\beta = 1$, then the normalization function $z(\mathbf{v})$ scales the vector \mathbf{v} along a ray to the origin, proportioning neural activity between the alternatives along the line:

$$\bar{z} = \sum_i z_i(\mathbf{v}) = \sum_i \frac{v_i}{\omega \sum_i v_i} = \frac{1}{\omega}. \quad (5)$$

¹⁰ The prevailing models of the comparison stage of the decision process (for example, the *drift diffusion model*, Ratcliff 1978) have been shown to yield a stochastic additive formulation (Webb 2019). Moreover, this process determines the density $f(\boldsymbol{\eta})$. For instance, it is broadly observed that as neural activity increases, the signal-to-noise ratio of decoded neural quantities also increases (e.g. McAdams and Maunsell 1999, Churchland et al. 2011). This is important because of a vast literature documenting that individual neural responses are approximately Poisson-like in their activity (Tolhurst et al. 1983). In terms of our model, this implies that the variance of $\boldsymbol{\eta}$ should not scale too strongly with \mathbf{v} , else choice might become *more* stochastic as valuations increase. Indeed, we will see that normalization can be interpreted as a specification of the variance of a choice model, thus imposes strong, testable, implications on choice data.

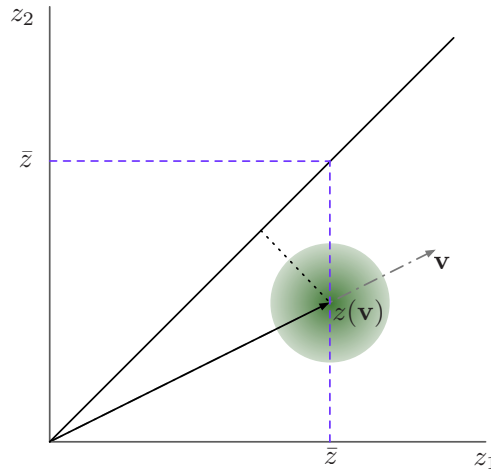


Figure 1 The transformation $z(\mathbf{v})$ for binary choice. The stochasticity in the comparison η is depicted by the shaded error density. Therefore the distance from the vector to the 45° line determines the probability that the alternative with the highest value is chosen, $\Pr[u_1 > u_2]$.

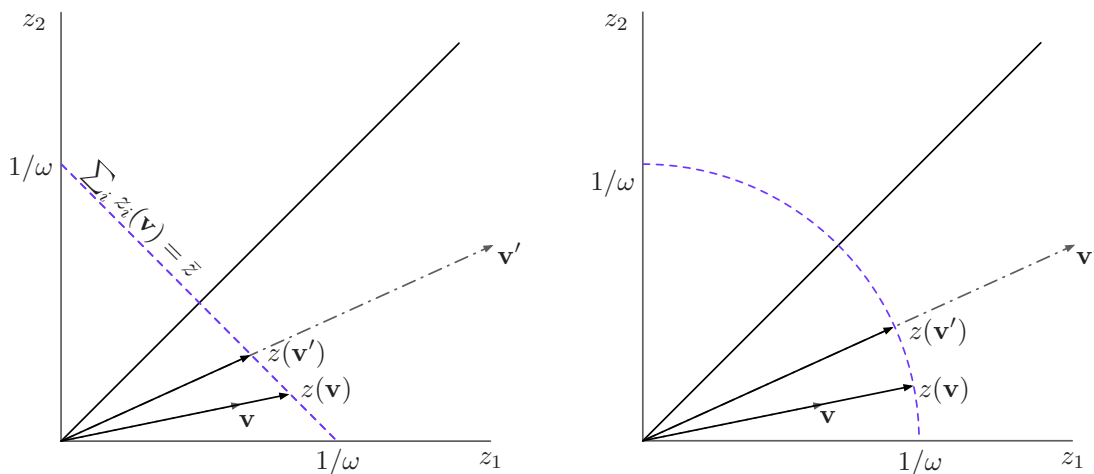


Figure 2 The proportionate scaling implemented by normalization for $\beta = 1$ (left) and $\beta = 2$ (right).

We now can reinterpret the bound \bar{z} as the ratio $1/\omega$, with ω determining the strength of the normalization (Figure 2). As $\omega \rightarrow 0$, the normalization term shrinks and along with it the means to bound $z(\mathbf{v})$.

For any $\beta > 0$, divisive normalization maps \mathbf{v} to a general class of geometric figures known as a *super-ellipse*. For instance, when $\beta = 2$, normalization scales the vector \mathbf{v} to the quarter-circle of radius $1/\omega$, since $z(\mathbf{v}) = \frac{1}{\omega} \frac{\mathbf{v}}{\|\mathbf{v}\|}$. Setting $\beta = 3$ maps \mathbf{v} to a hyperellipse, while $\beta = \infty$ maps to the square of size $1/\omega$ (see Figure 1). Notice that in each of these cases, divisive normalization preserves the relative magnitudes of the elements of \mathbf{v} and scales neural activity to the boundary determined by \bar{z} . Therefore divisive normalization implements a relative coding of value, subject to

the boundary constraint on neural activity. In the following sections, we will explore the patterns in choice behaviour generated by this relative coding of valuations.

3. Behavioural Implications of Normalization

The behavioural predictions of normalization stem from the interaction between scale and stochasticity that is typically present in discrete choice models (McFadden 2001, Train 2009). To explore these predictions, we incorporate the normalization equation (2) directly into (4):

$$P_i(z(\mathbf{v})) = \int \mathbf{1} \left[\frac{v_i - v_j}{\sigma + \omega (\sum_n v_n^\beta)^{\frac{1}{\beta}}} > \eta_j - \eta_i, \quad \forall j \neq i \right] f(\boldsymbol{\eta}) d\boldsymbol{\eta}. \quad (6)$$

In a model without normalization ($\omega = 0$), choice probabilities are given by a standard random utility formulation, thus the scale of the model is set by the variance of the stochastic term $\boldsymbol{\eta}$. For instance, when $f(\boldsymbol{\eta})$ is the density of the independent normal distribution, $\text{Var}(\eta_i)$ is typically assumed to be 1, and the parameter σ determines the variance of a binary Probit model: $\Pr[v_i - v_j > \sigma(\eta_j - \eta_i)]$. Note that this variance is constant over choice sets.

By contrast, introducing normalization scales the variance in a systematic manner proportional to the number and value of the alternatives in the choice set. This scaling depends on assumptions placed on the density $f(\boldsymbol{\eta})$, but for now, we simply maintain the standard assumption that $\text{Var}(\eta_i)$ is a constant. In an important respect, a distributional specification is also what we are proposing here. If one multiplied the denominator of the normalization equation (6) through to the right-hand side of the inequality, the distribution of the error $\boldsymbol{\eta}$ could be appropriately redefined to incorporate normalization, with the inequality in brackets in (6) given by: $\left[v_i - v_j > \left(\sigma + \omega (\sum_n v_n^\beta)^{\frac{1}{\beta}} \right) (\eta_j - \eta_i) \right]$.

Therefore value normalization is equivalent to specifying that the variance of the stochastic term in a discrete choice model depends on magnitudes in a particular manner. Recall that $i = 1$ denotes the highest valued alternative of a choice set. The following proposition states how the probability of choosing this alternative, P_1 , decreases in the magnitude of the valuations.

PROPOSITION 1 (Scaling of Choice Stochasticity). *For all \mathbf{v} and \mathbf{v}' such that $v_i - v_j = v'_i - v'_j$, and $v'_i > v_i, \forall i, j$, a normalized value function (2) implies that $P_1(z(\mathbf{v}')) < P_1(z(\mathbf{v}))$.*

Proof From (2),

$$|z_i(\mathbf{v}') - z_j(\mathbf{v}')| = \left| \frac{v'_i - v'_j}{\sigma + \omega (\sum_i v_i'^\beta)^{\frac{1}{\beta}}} \right| = \left| \frac{v_i - v_j}{\sigma + \omega (\sum_i v_i'^\beta)^{\frac{1}{\beta}}} \right| < |z_i(\mathbf{v}) - z_j(\mathbf{v})|.$$

Moreover, for the highest valued alternative,

$$\mathbf{1} [z_1(\mathbf{v}') - z_j(\mathbf{v}') > \eta_j - \eta_1] \leq \mathbf{1} [z_1(\mathbf{v}) - z_j(\mathbf{v}) > \eta_j - \eta_1], \forall \boldsymbol{\eta} \text{ and } \forall j \neq 1.$$

Therefore $P_1(z(\mathbf{v}')) < P_1(z(\mathbf{v}))$ from (4). \square

Some intuition for this scaling and its effect on choice behaviour can be observed in Figure 3. Consider two binary choice sets in which the difference between the valuations in each set are constant ($v_1 - v_2 = v'_1 - v'_2$), but the alternatives in one set are of higher value (i.e. $v'_i > v_i$). In an additive random utility model, the resulting choice probabilities in these two choice sets are equivalent (i.e. the vectors \mathbf{v} and \mathbf{v}' are equi-distant from the 45° line). But under normalization there is now an important distinction, the higher-valued alternative in each set is scaled more (in absolute terms) than the lower. Therefore the normalized valuations have a smaller *relative* ratio in the higher valued choice set — $z(\mathbf{v}')$ is closer to the 45° line than $z(\mathbf{v})$ — leading to increased choice errors.

A dependence between choice errors and the magnitudes of stimuli — not just their differences — has been routinely described in the psychology literature for nearly two centuries, codified as Weber’s Law (Weber 1834, Stevens 1961, Glimcher 2011).¹¹ In our model, such behaviour results directly from a constrained neural computation. However the departure of choice behaviour from a purely rational benchmark (of no choice errors) is implemented in a constrained-optimal manner.

PROPOSITION 2 (Divisive Normalization yields as few choice errors as possible). *For any \mathbf{v} , \bar{z} , and $\alpha > 0$ such that $\alpha v_i \leq \bar{z} \forall i$, then P_1 is maximal when $\alpha \mathbf{v} = z(\mathbf{v})$, $\omega = \frac{1}{\bar{z}}$, and $\sigma = 0$.*

The proof is provided graphically in Figure 3. Since Divisive Normalization scales \mathbf{v} directly to the bound constraint, not to some point interior, the distance between the vector $z(\mathbf{v})$ and the 45° line is as large as possible. Therefore, given the bound constraint, the probability of making an error is reduced as much as possible. This result also clarifies the normative implications of β . When $\beta > 1$, normalization maps the vector \mathbf{v} to a family of curves that lies outside the linear constraint. The smallest possible probability of an error occurs when $\beta = \infty$ and \mathbf{v} is mapped to a square.¹²

¹¹ Weber’s Law states that the change in a stimulus that will be *just noticeable* is a constant ratio of the original stimulus. Said differently, the (objectively measureable) difference between larger stimuli must increase for that difference to be perceptible to human subjects. Consider Weber’s original experiment. Each subject is given a 1kg sack of sand, referred to as the reference stimulus, then given a second “test” sack and asked to choose which is heavier. As the weight of the test sack increases, the likelihood that subjects choose the test sack increases. Now the experiment is repeated with a 10kg sack. Weber found that the range of weights over which subjects make an error increases in proportion to the weight of the reference sack.

¹² Our focus on choice errors follows the economic literature which has previously used errors as a metric of optimality (Robson 2001a, Rayo and Becker 2007, Robson and Samuelson 2010). While we do not argue explicitly in terms of the evolutionary criteria of “expected loss” which incorporates the magnitude of a choice error (Netzer 2009), in the appendix we show that the general divisive normalization computation does allow a degree of monotonicity in the transformation of subjective values, such that “more valuable” choice sets (in the sense that $\alpha \mathbf{v}$ is more valuable than \mathbf{v} if $\alpha > 1$) will lead to fewer errors than less valuable choice sets. Of course, a full normative treatment of the neural decision-making problem would require a complete accounting of the costs of decision-related errors to the chooser and the metabolic costs of relaxing the constraints we identify — on an evolutionary timescale.

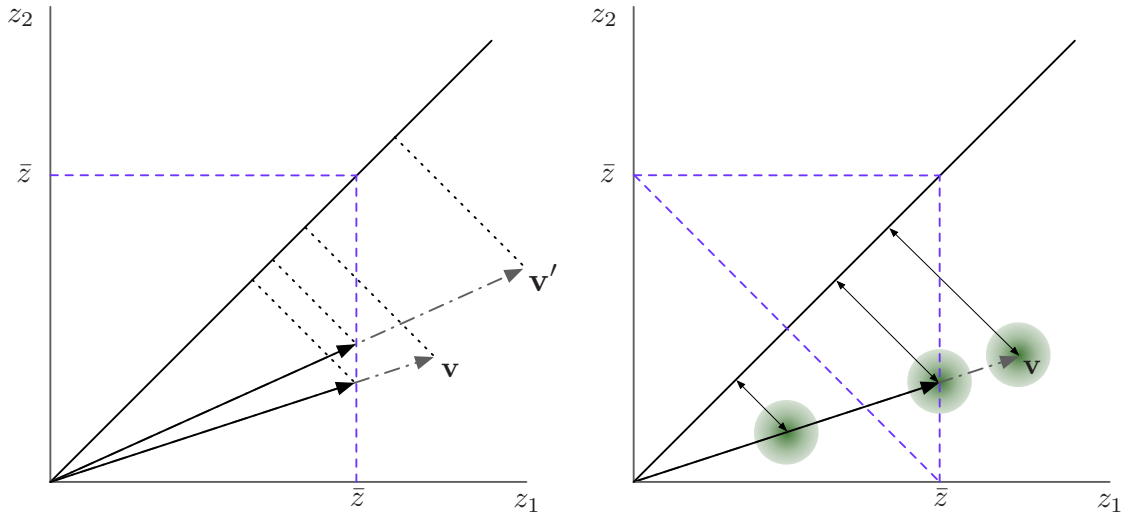


Figure 3 (Left) Choice stochasticity scales with value of the choice set. (Right) Divisive normalization scales \mathbf{v} to the bound constraint, minimizing choice errors given the bound constraint \bar{z} . Compare the scaling of \mathbf{v} to the bound \bar{z} versus a scaling to the interior of the bound.

3.1. Substitution Patterns and Violations of IIA

We now consider the patterns in choice behaviour when more alternatives are introduced into the choice set. Under Divisive Normalization, the neural activity for each alternative is re-scaled to abide by the bound constraint, proportionate to the value of new alternatives. Figure 4 depicts this result graphically for the addition of a third alternative (v_3) under the assumption of a linear constraint (i.e. a simplex in \mathbb{R}_+^3). As before, the highest-valued alternative is scaled more than the second, therefore the difference between $z_1(\mathbf{v})$ and $z_2(\mathbf{v})$ shrinks, and this scaling continues as the value of the third alternative is increased.

This pattern holds for choice sets of size N . For any choice set with valuations $\mathbf{v} \in \mathbb{R}_+^N$, define $\mathbf{v}_v \equiv [\mathbf{v}, v] \in \mathbb{R}_+^{N+1}$ as the valuation of a choice set which appends an alternative with valuation v .

LEMMA 1. A normalized value function (2) implies $|z_i(\mathbf{v}_{v'}) - z_j(\mathbf{v}_{v'})| < |z_i(\mathbf{v}_v) - z_j(\mathbf{v}_v)| < |z_i(\mathbf{v}) - z_j(\mathbf{v})|$, for all $i, j \leq N$, $j \neq i$, all $v' > v$, and all N .

Proof By definition, $\mathbf{v}_0 = [\mathbf{v}, 0]$ is the original vector \mathbf{v} , but in \mathbb{R}_+^{N+1} . For any $N \geq 2$, and all elements $i, j \leq N$,

$$\begin{aligned}
 |z_i(\mathbf{v}_{v'}) - z_j(\mathbf{v}_{v'})| &= \left| \frac{v_i - v_j}{\sigma + \omega \left(v'^\beta + \sum_n^N v_n^\beta \right)^{\frac{1}{\beta}}} \right| < \left| \frac{v_i - v_j}{\sigma + \omega \left(v^\beta + \sum_n^N v_n^\beta \right)^{\frac{1}{\beta}}} \right| = |z_i(\mathbf{v}_v) - z_j(\mathbf{v}_v)| \\
 &< \left| \frac{v_i - v_j}{\sigma + \omega \left(0 + \sum_n^N v_n^\beta \right)^{\frac{1}{\beta}}} \right| \\
 &= |z_i(\mathbf{v}_0) - z_j(\mathbf{v}_0)|. \quad \square
 \end{aligned}$$

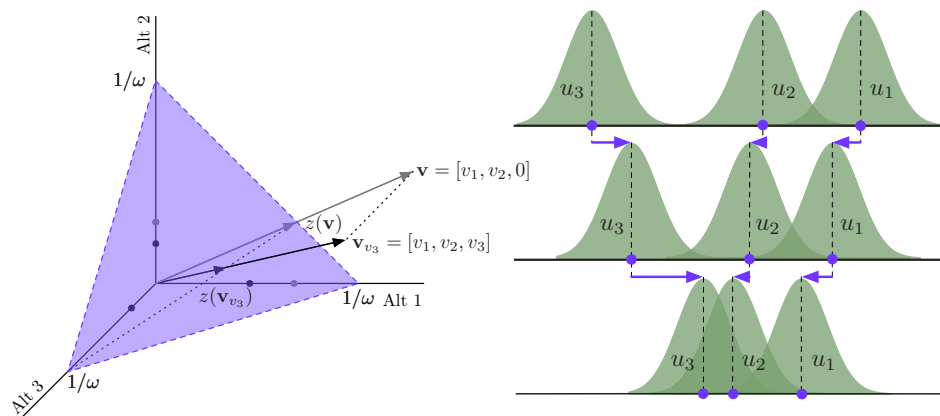


Figure 4 The introduction of a third alternative scales the valuations via the normalization equation and alters the relative likelihood of choosing between alternatives 1 and 2. The small circles represent the coordinates of the normalized vector $z(\mathbf{v})$.

The scaling described in Lemma 1, in which the difference between normalized valuations shrinks, is a critical feature of Divisive Normalization: it implies a decrease in the odds that alternative 1 is chosen relative to alternative 2 (i.e. the ratio $\frac{P_1}{P_2}$ decreases). Therefore substitution patterns induced by normalization depart from the IIA axiom in a testable manner.

To understand how, consider a model without normalization (i.e. $\omega = 0$ in equation 6). In this random utility model, substitution patterns are determined by the distribution of the error vector $\boldsymbol{\eta}$. For instance, when η_i follow the independent *Gumbel* distribution, we have the familiar Multinomial Logit (MNL) model with $P_i = \frac{e^{v_i}}{\sum_n e^{v_n}}$. The ratio $\frac{P_i}{P_j} = e^{v_i - v_j}$ does not depend on the valuations of the additional alternatives in the choice set, therefore satisfies IIA. By contrast, normalization predicts a decrease in the odds $\frac{P_1}{P_2}$, and this decrease is present even when the error distribution is Gumbel (see also Figure 5 and Appendix B).

PROPOSITION 3 (IIA Violations - Gumbel). For $v_i > v_j$, a normalized value function $z(\mathbf{v})$, and density function $f(\eta_i) = e^{-(\eta_i + e^{-\eta_i})}$, the introduction of a third alternative v yields relative choice probabilities $\frac{P_i(z(\mathbf{v}_v))}{P_j(z(\mathbf{v}_v))}$ which decreases in v .

Proof Consider two values of a third alternative, $v' > v$. Since $v_i > v_j$, then $\frac{P_i(z(\mathbf{v}_v))}{P_j(z(\mathbf{v}_v))} = e^{z_i(\mathbf{v}_v) - z_j(\mathbf{v}_v)} = e^{|z_i(\mathbf{v}_v) - z_j(\mathbf{v}_v)|} < e^{|z_i(\mathbf{v}_{v'}) - z_j(\mathbf{v}_{v'})|} = \frac{P_i(z(\mathbf{v}_{v'}))}{P_j(z(\mathbf{v}_{v'}))}$, for all i, j and all $v' > v$. \square

The patterns of IIA violations predicted by normalization depend on the distributional assumption we place on the stochastic term. If we instead assume an independent normal distribution for $\boldsymbol{\eta}$, the pattern of IIA violations predicted by normalization take a different form (Figure 5). As the value of a third alternative increases, the ratio $\frac{P_1}{P_2}$ still declines, but only until the third alternative starts capturing significant choice probability. Then the ratio $\frac{P_1}{P_2}$ increases and the first alternative is chosen relatively more often. Given the absence of a closed form for the normal distribution, a

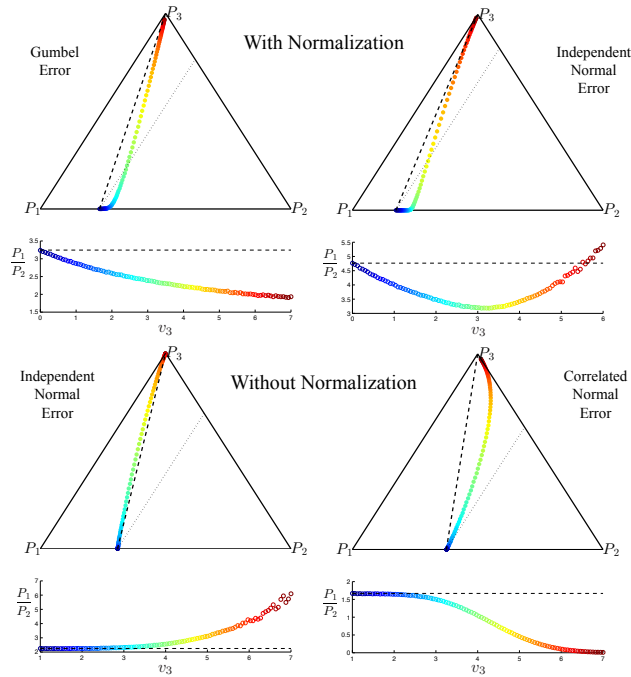


Figure 5 Simulated choice probabilities from a discrete choice model with and without normalization, as v_3 is varied. The IIA property is denoted by the dashed line.

formal statement along the lines of Proposition 3 is not possible, however intuition for this result can be found in Figure 4. As the density of u_3 shifts to the right, it overlaps substantially with the density of u_2 before that of u_1 . This sends the probability of choosing the second alternative quickly to zero, and results in a substitution pattern between alternatives which has a characteristic “u-shape” (Figure 5).

These behavioural predictions of Divisive Normalization naturally extend to larger choice sets. In a random utility model, adding new alternatives to the choice set will necessarily decrease the probability of choosing an existing alternative. This is because a new alternative has a positive probability of being chosen, no matter how small its value. However in a model with normalization, there is a second effect to consider. Increasing the number of choice alternatives changes the total value of the choice set thus requires neural activity to be re-proportioned (Figure 4). This scaling further depresses the probability of choosing the highest valued alternative and imposes a particular pattern on the choice probabilities of other alternatives. In section 4.2, we present a new behavioural experiment designed to test for the presence of normalization as the choice set grows, and to assess the ability of the normalization model to predict across experiments and subject samples.

3.2. Alternative Models of IIA Violations

Given the predicted substitution patterns of Divisive Normalization, it is important to consider the predictions of alternative models and how we might distinguish between them. For instance,

adaptations of the random utility model have been previously proposed in order to relax the IIA axiom, all working through the specification of the error distribution. Importantly, many of these alternative approaches are nested in our specification.

Luce Models If $\omega = 0$ and $f(\cdot)$ is the density of the independent Gumbel distribution, equation 6 reduces to the MNL model with variance proportional to σ^2 . This model imposes IIA on the data. If we maintain the Gumbel density but allow $\omega > 0$, the model 6 belongs to the class of “set-dependent Luce models” (Marley et al. 2008) which relaxes IIA but requires that relative log-odds ratios are still proportionate across choice sets (Appendix B).

Multinomial Probit If $\omega = 0$ and $f(\cdot)$ is the multi-variate normal density with a fully-parameterized covariance matrix, equation 6 is the multinomial Probit model. This flexible specification has led to the assertion that the MNP can “represent any substitution pattern” (Meyer 1991), though this is clearly too strong of a claim. For instance, substitution patterns which arise from a relationship between the variances of η_i and the magnitude of valuations in the choice set can not be captured. Since the lack of a closed-form expression prohibits a definitive statement of which substitution patterns the MNP can and cannot capture, the ultimate test of its limits will have to be empirical.

Range Normalization We also consider another class of models which normalize valuations by the range of alternatives (Padoa-Schioppa 2009, Soltani et al. 2012, Bushong et al. 2016). A Range Normalization model can implement a bounded value function, provided that the range of valuations is determined by all possible alternatives the decision-maker might encounter. Let \mathcal{V} be this “global” set of valuations (so $\mathbf{v} \subseteq \mathcal{V}$), and denote $\Delta\mathcal{V} \equiv \max\mathcal{V} - \min\mathcal{V}$ as the range of this set. The global range normalization function is then $z_i(\mathbf{v}) \propto \frac{v_i}{\Delta\mathcal{V}}$, by which every possible alternative is normalized on a line between $\frac{\min[\mathcal{V}]}{\Delta\mathcal{V}}$ and $\frac{\max[\mathcal{V}]}{\Delta\mathcal{V}}$. However this form of range normalization has a substantial empirical drawback. While its value function is bounded, it can not distort valuations when alternatives are varied within a choice set because $\Delta\mathcal{V}$ remains fixed over choice sets; when an alternative v_3 is added to the set, the normalized valuations $z_1(\mathbf{v})$ and $z_2(\mathbf{v})$ do not change.

For a range normalization model to generate substitution patterns, the range of the current choice set must be used. If we let $\Delta\mathbf{v} \equiv \max\mathbf{v} - \min\mathbf{v}$, then a “local” range normalization function is $z_i(\mathbf{v}) \propto \frac{v_i}{\Delta\mathbf{v}}$.¹³ This function, however, is not bounded. To see why, consider a binary choice set in which v_1 and v_2 are close together. As the range between v_1 and v_2 shrinks, the normalized valuations $z_i(\mathbf{v}) \rightarrow \infty$. Unboundedness is obviously an unappealing property of a model attempting to incorporate constraints on the range of neural activity. Nevertheless, we might still consider the predictions of this unbounded model as additional alternatives are added to the choice set. In

¹³ Other examples of models which use local range normalization include Wilcox (2011).

particular, as v_3 grows, the range $\Delta \mathbf{v}$ will shrink, magnifying the difference between z_1 and z_2 . In a probabilistic model, this will increase the probability that the highest-valued alternative is chosen. Note that this is the opposite prediction of the value normalization model in Section 3.1.¹⁴

There is one additional observation to make about the relationship between a normalization model and existing models in the literature. If normalization influences choice behaviour, the model estimates of MNP (or any model without normalization) will be inconsistent. For intuition, it is helpful to consider normalization as a form of heteroskedasticity in the discrete choice model (6), in which the variance is modulated by the elements of the choice set. In contrast to linear models, heteroskedasticity in non-linear discrete choice models yields both inefficient *and* inconsistent estimates (Greene 2003). Therefore, if there is indeed normalization present in these datasets, interpreting the estimates from models that explicitly rule out normalization will be problematic. This provides further justification for including normalization in the model specification.

4. Choice Experiments

We now turn to the empirical evidence for how valuations are normalized by the choice set. To test such predictions in a behavioural setting, Louie et al. (2013) developed a two-stage valuation and choice task over common snack-food items. The first stage of the experiment elicited a willingness-to-pay (bid) for each item using an incentive-compatible auction mechanism (Becker et al. 1964), which we denote $\mathbf{b} = [b_1, \dots, b_N]$. This yields a measure of value for each item in the experiment that is taken *independently* of the other items. In the second stage, subjects then chose a single alternative from choice sets comprised of subsets of these items. Divisive normalization describes how valuations are transformed by the choice set, thus predicts substitution patterns between alternatives when the value and composition of a choice set is varied.

To assess and compare the substitution patterns predicted by Divisive Normalization, Range Normalization, and other competing models, we analyze both the original dataset from Louie et al. (2013) for trinary choice sets and present data from a new experiment which varies the size of the choice set. In both datasets, we aim to test the model using purely behavioural measures, therefore the incentive compatible bids \mathbf{b} are used as an independent measurement of \mathbf{v} .¹⁵ Recall that our aim is to assess how valuations, at the time of choice, are transformed by the context of a choice set via the normalization function $z(\cdot)$. Variation in the independent measures (\mathbf{b}) across choice

¹⁴ A restricted form of normalization model rectifies the unboundedness problem by setting $\min[\mathbf{v}] = 0$ (e.g. González-Vallejo 2002). This model also provides a link between range normalization and divisive normalization. To see how, recall that as $\beta \rightarrow \infty$, the β -norm converges to a maximization. Therefore $z_i(\mathbf{v}) \propto \frac{v_i}{(\sum_n v_n^\beta)^{\frac{1}{\beta}}} \rightarrow \frac{v_i}{\max[\mathbf{v}]}$. The divisive normalization computation therefore simplifies to this restricted form when β is large.

¹⁵ In Appendix ??, we assess whether any biases in the independent bids could possibly generate the substitution patterns we observe. We find that this explanation is highly unlikely given the pattern of bids.

sets will allow us to examine the substitution patterns that emerge in choice probabilities via $z(\mathbf{b})$, both non-parametrically and with a structural estimation of the Divisive Normalization model.

A structural analysis is particularly useful because it allows us to compare the Divisive Normalization model to its competitors across experimental designs. One of the benefits of a structural model is that parameter estimates from one dataset can be used to predict behaviour in another dataset. If the distribution of subject-level parameters is stable across different samples, and if the model is indeed an accurate reflection of behaviour, then the normalization parameters from one dataset should provide a good prediction of behaviour in another dataset. All analyses reported in this section are novel, unless specifically noted.

4.1. Tertiary Choice Experiment

In the original experiment conducted by Louie et al. (2013), 40 healthy volunteers (21 female, ages mean age 23.0 years) with normal or corrected-to-normal vision participated in the experiment after giving informed consent. Subjects were instructed to fast for 4h before the experimental session and informed that they would have to remain for 1h after the completion of the session, during which the only food they could consume was any food items received from the experiment.

In the first stage of the experiment, each subject performed 60 bid trials to establish subject-specific valuations for the array of experimental goods. In each bid trial, subjects viewed a picture of a single snack food item and reported their willingness-to-pay for that item using a mouse-controlled slider bar (\$0-\$4 in \$0.01 increments). The stimuli consisted of 30 different snack foods presented as high-resolution color images (110 pixels per inch) on a black background; the full list of snack foods and two example images are presented in Appendix D. Other than the visual image, no other information about the snack food was provided to the subject. Items were presented in randomized order, and each individual item was presented twice.

To implement incentive compatibility, each subject was endowed with \$4, and if a bid trial was chosen for realization at the end of the session, the outcome was determined via an auction mechanism (Becker et al. 1964).¹⁶ Each of 30 items was shown twice in a randomized order, and multiple bids for the same item were highly correlated ($\rho = 0.9105$, $p < 0.001$, Figure 6). For each subject, each item was then ranked according to its mean bid (Figure 6, Right).

¹⁶ Briefly, to realize a bid trial, subjects drew a chip from a bag containing chips numbered from \$0 - \$4 in \$0.10 increments; the drawn number determined the price p of the item in that trial and was compared with the bid b . If $b \geq p$, the subject received the item for the price p ; if $b < p$, the subject paid nothing and did not receive the item. Thus, it is incentive-compatible for a subject to report their maximal willingness-to-pay because they can not influence the price. Subjects were carefully informed of this property of the BDM auction in the initial instructions and practiced it before the actual experiment. At the conclusion of the experiment, a single trial from the session (bid or choice) was randomly selected for realization and the subject received their choice on that trial. In addition, each subject received a \$40 show-up fee.

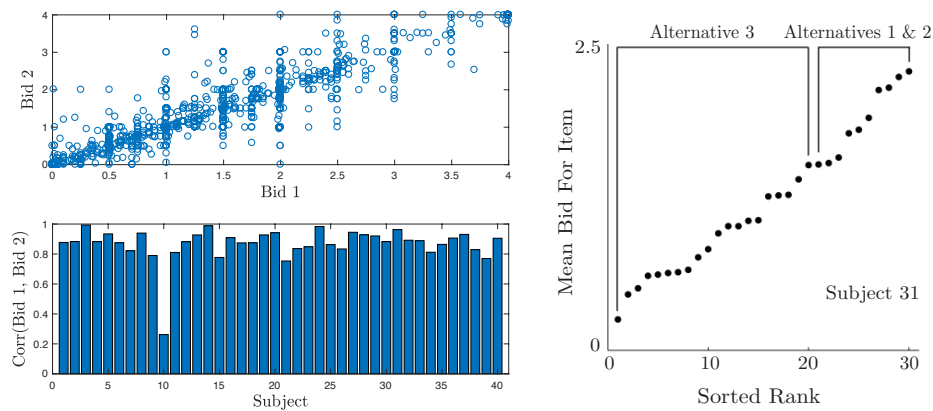


Figure 6 Top Left: The bids for each item and subject. Bottom Left: The correlation coefficient for each subject. Right: Ranked bids from an example subject.

In the second stage of the experiment, subjects performed choice trials from 250 unique choice sets composed of three alternatives. Choice trials were presented without a time limit and subjects were free to select an item as soon as the choice set was displayed; mean trial length was 2.4s, and each trial was followed by an inter-trial interval consisting of a blank screen for 1-1.5s. Each trinary set randomly sampled two alternatives from the 10 highest-valued items (termed alternatives ‘1’ & ‘2’ according to their rank order), and one alternative sampled uniformly from the 20 lowest-valued items (termed alternative ‘3’). Each presented triplet was sampled without replacement and the location of each item on the screen (left, middle, or right) was randomly assigned in each trial. Importantly, this process creates substantial variation in the alternatives labelled ‘1’, ‘2’, and ‘3’ on each trial. In fact, on different trials the same item can be labelled a ‘1’ or a ‘2’, depending on the value of the other alternatives. This provides a strict test of the normalization model since it is unlikely that other properties of individual items are driving the results, as described in Appendix ??.

For each alternative in the choice set, the mean of the two bids is denoted b_i , where i is the rank-order of that item in a particular set. To facilitate comparison across subjects in the reduced form analysis, we also report the bid for each item *relative* to the mean bid for all items (within a subject) as the variable \tilde{b}_i . Figure 7 reports the choice probabilities across the deciles of all bids, as well as a linear fit over all bids. As might be expected, the choice probabilities increase in the magnitude of the bids.¹⁷

4.1.1. Reduced Form Analysis We begin our analysis with a comparison of the observed choice frequencies across subjects. Due to heterogeneity in preferences, each subject’s bid distribution for the 30 items varied widely. For some subjects, bids for the items that comprise alternative

¹⁷ The weak relationship between b_2 and \hat{P}_2 is a property of the experimental design. Since $b_2 < b_1$ by definition, b_1 tends to be larger as b_2 increases, limiting any increase in the observed frequency of choosing the 2nd alternative, \hat{P}_2 .

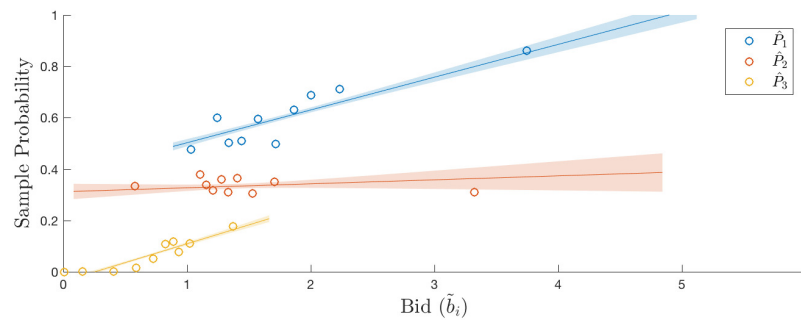


Figure 7 The sample choice probabilities of each alternative at the deciles of all bids. A linear fit over all bids is also depicted.

3 can be close to those for alternatives 1 and 2, while for other subjects, they can be substantially lower. This across-subject variation provides our first test. Under normalization, we should expect to see lower odds of choosing alternative 1 vs. 2 for subjects with higher bids for alternative 3.

This is indeed the case. Figure 8 reports the subject-level sample probabilities \hat{P}_1 , \hat{P}_2 , \hat{P}_3 across all choice sets, ordered by the average \tilde{b}_3 of each subject. A linear regression on the probabilities for each alternative is also depicted. Not only does the choice ratio between alternatives 1 and 2 decrease, but the probability that alternative 2 is chosen (\hat{P}_2) increases by ~ 0.19 as the average \tilde{b}_3 increases ($p < 0.043$, two-tailed).¹⁸ Across the sample, the ratio in which subjects select the highest and second-highest alternative decreases by a factor of 2.5 when the value of the third-highest alternative is increased. Subjects who tended to have higher valued 3rd-ranked items chose their highest-ranked items nearly 20% less frequently, and chose their second highest-ranked item nearly 15% more often.

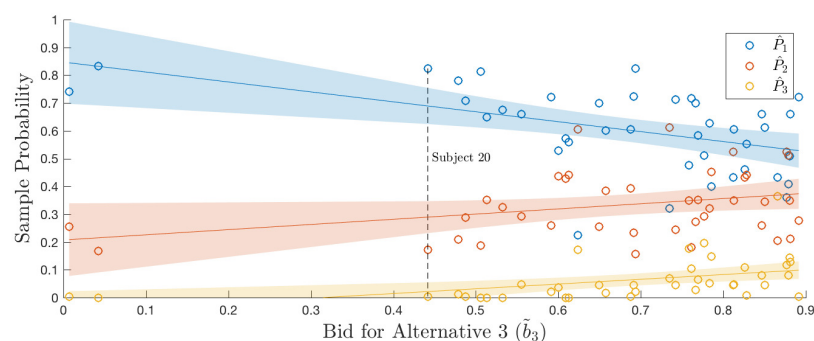


Figure 8 The sample choice probabilities of each alternative plotted across subjects by the average \tilde{b}_3 for each subject. Subject 20 is depicted as an example.

While an across-subject result is suggestive, the critical prediction is normalization at the trial-level depending on each subject’s evaluation of the choice set encountered. For instance, note that

¹⁸ This result is robust to the two outlier subjects with small average \tilde{b}_3 .

the above pattern could arise if, by chance, subjects in our sample with a larger average \tilde{b}_3 also tend to have smaller value differences between the top two alternatives ($\tilde{b}_1 - \tilde{b}_2$). The Divisive Normalization model introduced in Section 3 controls for this issue by allowing the choice set on a given trial to determine the relative choice probabilities. Before we address the performance of this model however, it is useful to consider an analysis introduced in Louie et al. (2013) which coded the bid of alternative 3 relative to the mean value of alternatives 1 and 2 on each trial ($b_3 - \frac{b_1+b_2}{2}$). This metric alleviates issues with differing bid ranges across subjects by focusing solely on the composition of the set on each trial. The analysis then dropped the small number of trials in which alternative 3 was chosen, and a logit choice model was fit to the remaining data segregated into five bins of ($b_3 - \frac{b_1+b_2}{2}$). Relative preference is therefore inferred from a binary choice between the alternatives 1 and 2 (within a bin of alternative 3), controlling for differences in valuations of the top two alternatives. The magnitude of a logit parameter (the “steepness” of the logistic function) therefore gives a measure of the ratio $\frac{P_1}{P_2}$ at the mean value for $b_1 - b_2$. Essentially, this method assumes that IIA holds “locally” within a bin in order to assess whether it is violated “globally” over bins.

Figure 9 reports two measures of the probability ratio $\frac{P_1}{P_2}$. The first is the ratio of the raw sample probabilities over the top two alternatives $\frac{\hat{P}_1}{\hat{P}_2}$, binned over the quintiles of the bids for the 3rd alternative in the set. The second is the main result reported by Louie et al. (2013). In both analyses, the relative probability of choosing the highest ranked item significantly decreases as the value of alternative 3 approaches the top two alternatives. There is also evidence for a “u-shape” in relative choice probabilities; the probability ratio between alternatives 1 and 2 rises as the third alternative reaches the average for the top two. This substitution pattern is consistent with a normalization model with a normal distribution for $\boldsymbol{\eta}$, as described in section 3.1. We will now examine the form of this normalization, whether existing models can also capture it, and whether it is robust across experimental paradigms.

4.1.2. Estimation Results and Model Comparison — Pooled We now turn to estimation of the Divisive Normalization model introduced in Section 3 and a comparison with three alternative specifications: the Multinomial Logit (MNL), Multinomial Probit (MNP), and Range Normalization model defined in Section 3.2. To compare these models, we restate (6) in terms of the observed bids and with the weights in the normalization pool restricted to be identical (i.e. $\omega_i = \omega$).

$$P_i(\mathbf{b}) = \int \mathbf{1} \left[\frac{b_i - b_j}{\sigma + \omega \left(\sum_n b_n^\beta \right)^{\frac{1}{\beta}}} > \eta_j - \eta_i, \quad \forall j \neq i \right] f(\boldsymbol{\eta}) d\boldsymbol{\eta}. \quad (7)$$

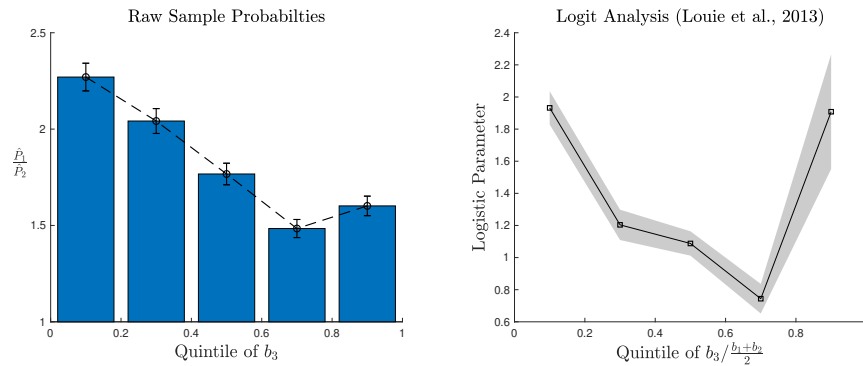


Figure 9 (Left) The ratio of the sample probabilities for the top two alternatives, binned over the quintiles of the third alternative. (Right) The coefficient from a logistic fit of choice between the top two alternatives, over the range of the third alternative in the set (normalized on each trial), reported by Louie et al. (2013).

This specification (7) has an important property; the parameter ω measures the influence of the choice set composition on overall variance. Since a null hypothesis of $\omega = 0$ nests the MNP and MNL, it therefore yields a nested log-likelihood ratio test for the presence of normalization in a dataset. We begin with a pooled analysis on the full dataset (250 trials \times 40 subjects = 10000 observations) and describe each of these models in turn.

Divisive Normalization We estimate three different specifications allowing the variance in the model to be determined by the value of alternatives in the choice set (i.e. $\omega \geq 0$):

- To verify that substitution patterns in the dataset can be captured solely by Divisive Normalization, we restrict $\beta = 1$ and the covariance matrix of $\boldsymbol{\eta}$ to be independent normal (parameterized by its Cholesky decomposition: $l_{2,2} = 0.866$, $l_{2,1} = 0.5$).¹⁹ In this specification, σ represents the constant portion of the variance, while the term governed by ω represents the normalized portion of the variance. This is the original model proposed by Louie et al. (2013).
- To determine the form of Divisive Normalization and how it compares to the MNP, we relax the restriction on β for a total of three parameters (σ, ω, β) . This specification has the same number of parameters as the MNP.
- Finally, we estimate a full specification that nests both Divisive Normalization and the MNP. This specification unrestricts the covariance matrix for $\boldsymbol{\eta}$ parameterized by $l_{2,1}$, $l_{2,2}$, for a total of five parameters $(\sigma, \omega, \beta, l_{2,1}, l_{2,2})$.

In each of these specifications, if we find our estimate of ω to be significantly positive, we can reject a model with constant variance in favour of a model with normalization.²⁰ Model estimates

¹⁹ The multivariate normal distribution is parameterized with the constant variance term σ and the Cholesky factorization of the covariance matrix, differenced with respect to the first alternative, $(l_{2,1}^1 \ l_{2,2}^0)$.

²⁰ Each specification is estimated via Maximum Likelihood with bound constraints to ensure that the parameters σ , ω , and β were non-negative.

are reported in columns 4–6 of Table 1. In each of the Divisive Normalization specifications, we find our estimate of ω is significantly greater than zero ($p < 0.001$, LR test). This suggests that the composition of the choice set affects the degree of variance in choice behaviour — and therefore the relative probabilities — in a manner consistent with the normalization model presented in section 3.²¹

Multinomial Probit To determine whether the MNP can capture the substitution patterns we observe in this dataset, we also estimated the MNP model ($\omega = 0, \beta = 1$) with an unrestricted covariance matrix, for a total of three parameters ($\sigma, l_{2,1}$, and $l_{2,2}$), reported in column 3 of Table 1. The log-likelihood of the MNP was lower than each of our restricted normalization specifications, the BIC was higher, and a non-nested likelihood ratio test (Vuong 1989) rejects the MNP in favour of the three-parameter normalization specification with an independent covariance matrix ($p < 0.001$). Not surprisingly, the worst performing specification was the MNL since it imposes IIA.

Range Normalization To estimate the Range Normalization model, we replace the divisive normalization term in the denominator of (7) with its counterpart for range normalization that is “local” to the choice set: $\sigma + \omega(\max \mathbf{b} - \min \mathbf{b})$. The baseline specification of this model has two free parameters, σ and ω , which again govern the constant and normalized portion of the variance, respectively. We also estimate a full specification with an unrestricted covariance matrix, for a total of four parameters. The Divisive Normalization specification outperforms both specifications of the Range Normalization model in terms of a larger log-likelihood and a smaller BIC (columns 9 and 10 of Table 1).

To gauge why the divisive normalization model yields this improvement in fit, we analyzed the predicted probabilities from each of these models using the reduced form analysis from Louie et al. (2013). Given the estimates in Table 1 and the bids for each subject, we simulated choice data from each of the models and conducted the logistic analysis described in Section 4.1.1. The results are reported in Figure 10. Only the Divisive Normalization model is able to capture the “u-shape” choice probability ratio observed in the data, with the minimum of this ratio determined by the magnitude of β . In contrast, both the MNP and the Range Normalization model predict that this ratio should increase as the bids for the 3rd alternative increases.

Finally, we used the estimated BIC for each model to approximate the posterior model probabilities across subsets of models (e.g. Wasserman 2000, Hawkins et al. 2015). We considered three subsets: models which simply allow normalization vs. not ($\omega = 0$ or $\omega \geq 0$), models which allow

²¹ To test the importance of the normal density assumption, we also examined a Divisive Normalization model ($\omega \geq 0$) in which $f(\cdot)$ is the Gumbel density (not reported in Table 1). We find that $\hat{\omega}$ is significantly different from zero with a log-likelihood of -7999.58. However it is the worst performing normalization specification, likely due to the fact that it cannot capture the shape of the $\frac{P_1}{P_2}$ ratio (Figure 5).

Table 1 Estimates of the Divisive Normalization model and alternative specifications for the trinary choice experiment. Standard errors are in parenthesis. Restricted parameters are in red. A ‘-’ represents parameters not present in the specification. The reported Posterior Model Probabilities are for i) models which simply allow normalization vs. not ($\omega = 0$ or $\omega \geq 0$), ii) models which allow different forms of normalization (e.g. $\beta > 0$, $\omega_i \neq \omega$), iii) models which un-restrict the covariance matrix of η , and iv) all models considered.

	MNL	Probit	MNP	Divisive Normalization					Range	
				Symmetric	Recurrent	Weights	Asymmetric	Weights	Normalization	
$\hat{\sigma}$	0.880 (0.036)	0.996 (0.004)	1.493 (0.053)	0.114 (0.024)	0.012 (0.022)	0.121 (0.049)	0.056 (0.026)	0.027 (0.025)	0.439 (0.028)	0.977 (0.100)
$\hat{\omega}$	0	0	0	0.177 (0.007)	0.412 (0.014)	0.183 (0.051)	0.032 (0.007)	0.214 (0.045)	0.370 (0.023)	0.252 (0.050)
$\hat{\omega}_i$	-	-	-	-	-	-	0.177 (0.003)	0.303 (0.048)	-	-
$\hat{\beta}$	1	1	1	1	25.74	0.723 (0.135)	1	3.458 (0.865)	-	-
$\hat{l}_{2,2}$	-	0.866	0.792 (0.033)	0.866	0.866	0.780 (0.044)	0.866	0.866	0.866	0.749 (0.044)
$\hat{l}_{2,1}$	-	0.5	0.431 (0.022)	0.5	0.5	0.454 (0.029)	0.5	0.5	0.5	0.513 (0.030)
LL	-8190.54	-8153.55	-7969.81	-7944.39	-7881.25	-7803.86	-7874.29	-7865.20	-8035.61	-7955.42
BIC	16390	16316	15967	15907	15790	15654	15776	15767	16089	15948
LRT of $\hat{\omega} = 0$ (p-value)				0.000	0.000	0.000	0.000	0.000	0.000	0.000
i. Posterior Model Prob.		0.000		1.000					0.000	
ii. Posterior Model Prob.		0.000			0.000			1.000	0.000	
iii. Posterior Model Prob.			0.000			1.000				0.000
iv. Posterior Model Prob.	0.000	0.000	0.000	0.000	0.000	1.000	0.000	0.000	0.000	0.000

variation in the form of normalization (e.g. $\beta > 0$, $\omega_i \neq \omega$), and models which un-restrict the covariance matrix of η . We also calculated posterior model probability across all models considered. Given the substantially smaller BIC for the Divisive Normalization model(s) compared to Range Normalization and the MNP, each of these analyses places a posterior model probability near one on a Divisive Normalization model.

4.1.3. Asymmetric Recurrent Weights in Normalization There is good reason to believe that recurrent connections in divisive normalization might be stronger than inhibitory connections (Carandini et al. 1997, Rust et al. 2006). If this is the case for the normalization of valuations, relaxing this restriction will result in a better fitting model. Therefore we also considered a Divisive Normalization specification which allows ω_i , the recurrent weight for alternative i , to differ from the weights for all other alternatives. The estimated specification is given by (7) with the normalization function replaced by

$$z_i(\mathbf{b}) = \frac{b_i}{\sigma + \left(\sum_{n \neq i} \omega b_n^\beta + \omega_i b_i^\beta \right)^{\frac{1}{\beta}}}. \tag{8}$$

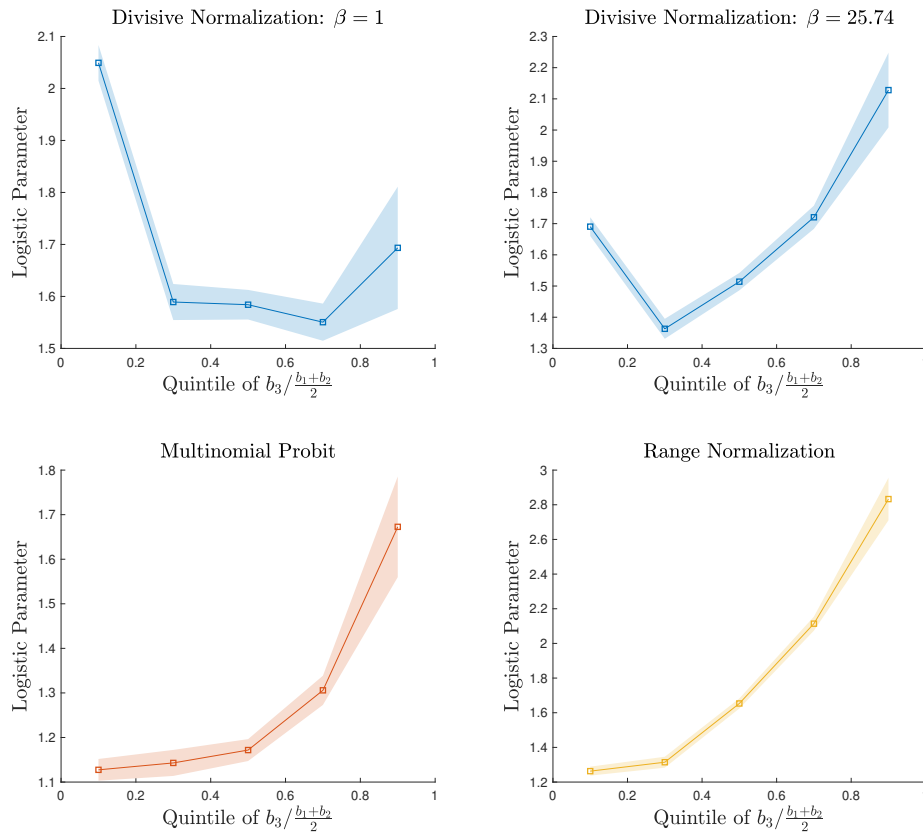


Figure 10 The logistic analysis from Louie et al. (2013), repeated on simulated data given the parameterizations estimated in Table 1.

A model which unrestricts the recurrent weights may also provide a better estimate of β . If the recurrent weight ω_i is larger than for the inhibitory pool, ω , then the denominator for the 1st alternative will largely be driven by this maximal value. However a model which artificially restricts these weights might then yield an estimate for β which is too large. Recall that when $\omega = \omega_i$, as β grows large the β -norm approaches a max operator thus closely approximates the normalization equation $z_i(\mathbf{b}) \propto \frac{b_i}{\max[\mathbf{b}]}$ (see Section 3.2).

Indeed, this is what we observe in the estimation results (columns 7 and 8 in Table 1). When the weights are restricted to be identical ($\omega_i = \omega$), the estimate of β is significantly larger than 1 ($p < 0.001$, LR test), therefore the variance in this specification is driven primarily by the highest valued alternative.²² While a large value for β is not implausible (recall that it simply reflects the form of the bound constraint on neural activity, thus need not be “computed” in any formal sense), we should note that the point estimate of β becomes quite imprecise when it is large. This

²² The LR statistic is calculated from the simple normalization model (with $\beta = 1$). In the specification with an unrestricted covariance matrix we cannot reject the hypothesis that $\beta = 1$ ($p = 0.09$, LR Test).

is because a given change in a large β yields little change in the choice probabilities for a typical choice set in our experiment, thus little change in the log-likelihood.²³

However when this restriction on the weights is relaxed, the denominator for each alternative is allowed to vary. We find that both the estimate for the recurrent weight is significantly larger than that of the inhibitory pool ($\hat{\omega}_i > \hat{\omega}$) and our estimate $\hat{\beta} = 3.458$ now lies within the range typically observed in sensory systems (a LR test of $\beta = 1$ is rejected, $p < 0.001$). The Log-likelihoods of these specifications are also larger than the other specifications, save for the full normalization specification with an unrestricted covariance matrix.

To summarize our results so far, we find the normalization model outperforms both a standard MNP model and a Range Normalization model in the pooled dataset. Our estimates of ω suggest that normalization is driving the variance of the choice model (therefore the resulting choice probabilities), and that the weight on the recurrent alternative ω_i is larger still. Our estimates on the form of the normalization constraint suggest that β lies within the realm typically observed in sensory systems, but estimates becomes less precise as β increases.

4.1.4. Estimation Results and Model Comparison — Modelling Heterogeneity To assess how well the Divisive Normalization can model the behaviour of a random participant in our sample, we also considered a random-coefficients specification of equation 7 in which the normalization parameter for each subject ω_s is drawn from the Gamma density $g(\omega_s; a, d)$ with shape parameter a and scale d . The probability of observing the sequence $\{i_1, \dots, i_T\}$ of $T = 250$ choices for each subject s is then

$$\int \prod_{t=1}^T P_{i_t}(\mathbf{b}|\omega_s) g(\omega_s; a, d) d\omega_s. \quad (9)$$

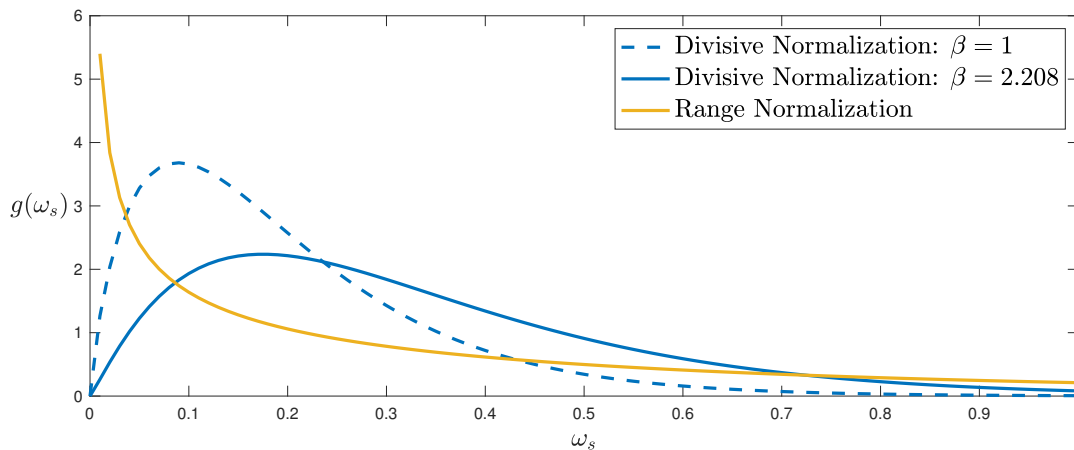
The likelihood of observing each sequence for each subject in the sample can then be maximized using standard simulation techniques (Train 2009). Results from this analysis are reported in Table 2 and the estimated density of ω_s for both Divisive Normalization and Range Normalization models are depicted in Figure 11.

The use of the Gamma distribution is particularly informative because it can place substantial density on $\omega = 0$ if the shape parameter a is small. For the Divisive Normalization model, we find that a is significantly different from zero and that the estimated density of ω_s places substantial

²³ Formally, there is a ridge in the log-likelihood function for values of β larger than ~ 10 , which makes the point estimate of a large β imprecise. Some intuition can be found in Figure 3. As β varies, there is little change in the geometric shape implied by normalization (e.g. a normalization boundary just inside the square would imply only a small change in z_1 and z_2). This implies only a small change in the resulting choice probabilities as the estimator varies β . To calculate the standard errors of $\hat{\omega}$ and $\hat{\sigma}$ in this specification, we hold $\hat{\beta}$ fixed at the reported estimate which yields a likelihood ratio statistic $\chi^2(LR, 1) = 0.05$. All reported hypothesis tests on normalization parameters are based on a likelihood ratio (LR) test statistic, not the reported standard errors.

Table 2 Random coefficient model estimates for the trinary choice experiment.

	Divisive Normalization		Range Normalization
\hat{a}	1.823 (0.355)	2.115 (0.422)	0.523 (0.143)
\hat{d}	0.108 (0.025)	0.1569 (0.050)	0.945 (0.306)
$\hat{\sigma}$	0.069 (0.027)	0.049 (0.327)	0.397 (0.021)
$\hat{\beta}$	1	2.208 (1.359)	-
LL	-7541.95	-7538.88	-7620.70
BIC	15112	15115	15269
Posterior Model Prob.	0.823	0.177	0.000

**Figure 11** The Probability Density of $\omega_s \sim \text{Gamma}(a, d)$ estimated from the trinary experiment.

weight on $\omega_s > 0$ for both specifications considered (with $\beta = 1$ and unrestricted). The estimate of β is again within the range typically observed in sensory systems. By contrast, the estimated density for the Range Normalization model places much more weight on $\omega_s = 0$. Finally, we find that the Divisive Normalization specifications have a larger log-likelihood and a smaller BIC compared to Range Normalization.

4.2. Set Size Experiment

The Divisive Normalization model makes additional predictions about how choice probabilities should change as the set size increases. An increase in the number of choice alternatives increases the total value of the choice set, thus re-proportions valuations according to the number of items in the set (Figure 4). This depresses the probability of choosing the highest-valued alternative relative to a random utility model. To test for this predicted pattern, we developed a two-stage experimental design which varies the size of the choice set.

This experiment also allows us to examine the robustness of our proposed Divisive Normalization model. One of the benefits of structural estimation is that, in principle, the distributions of structural parameters should be invariant. We can therefore examine how well the parameters from the trinary experiment, estimated via the structural specification (7), are able to capture the choice behaviour of a new set of subjects performing a different experiment.

4.2.1. The Set Size Task Our set size task had a similar structure to the trinary choice experiment. In the initial valuation stage, 30 subjects (11 female, mean age 24.4 yrs) reported their maximum willingness-to-pay for 30 individual snack food items, twice each (60 trials total). For each subject, items were then ranked according to their mean bid value, and the 10 highest-valued and 10 lowest-valued items were selected for inclusion in the second stage of the experiment.

In the second stage, subjects performed 270 choice trials from choice sets of varying sizes. On each trial t , a choice set consisted of two high-value alternatives (again, denoted alternatives ‘1’ & ‘2’ in rank-order) and a variable number of randomly chosen low-valued items for a total set size of $N_t \in \{2, 4, 6, 8, 10, 12\}$ items. Choice sets were constructed to include varying target value differences, with 45 different trials in each set size condition. On a given trial, item images were randomly assigned to one of 12 possible locations on the computer screen. Subjects were free to select an item as soon as the choice set was displayed and there was no time limit for making a selection; mean trial length was 3.1 s, and each trial was followed by an inter-trial interval consisting of a blank screen of 1-1.5 s. The remainder of the experimental design, including payment methods, were identical to the trinary choice experiment.

4.2.2. Estimation Results and Model Comparison — Pooled As expected, increasing the size of the choice set decreases the probability that the highest ranked alternative is chosen. In our largest set size of 12 alternatives, this probability decreases by 20% (Figure 12). Of course, any random utility model will have this qualitative feature. Therefore to determine if this decrease is better captured by a choice model with normalization, it is crucial to use a structural specification which controls for the size and valuations of the items in the set. To do so, we estimate the normalization model (6) with the only difference lying in the number of choice elements, N_t , now varying over trials. This yields the choice probabilities on trial t ,

$$P_{i,t}(\mathbf{b}) = \int \mathbf{1} \left[\frac{b_{i,t} - b_{j,t}}{\sigma + (\sum_{n \in N_t - 1} \omega b_{n,t}^\beta + \omega_i b_{i,t}^\beta)^{\frac{1}{\beta}}} > \eta_{j,t} - \eta_{i,t}, \quad \forall j \neq i \right] f(\boldsymbol{\eta}_t) d\boldsymbol{\eta}_t. \quad (10)$$

As in the trinary case, we initially restrict $\omega_i = \omega$ to provide a nested hypothesis test of the standard Probit model. Since the number of alternatives differs over trials, we restrict the covariance matrix of $\boldsymbol{\eta}$ to be independent normal. This also allows a direct comparison with the estimates from the same specification in the trinary experiment reported in Section 4.1.2.

The resulting maximum likelihood estimates for the entire pooled sample are reported in Table 3 for five nested specifications: the Probit, the simple normalization model proposed by Louie et al. (2013), a normalization model with β unrestricted, and two specifications which relax restrictions on ω_i . We also estimate a Range Normalization model as in Section 4.1.2.

Table 3 Maximum likelihood estimates for set size experiment. Restricted parameters are denoted in red, including parameter values taken directly from the trinary experiment in Table 1. The reported Posterior Model Probabilities are for i) a comparison of Divisive Normalization with the model fits from the trinary experiment, and ii) all models fit on the set size data.

	Probit	Divisive Normalization						Range Normalization
		Symmetric Weights		Asymmetric Weights		From Trinary		
$\hat{\sigma}$	1.210 (0.016)	0.985 (0.042)	0.001 (0.009)	0.022 (0.011)	0.000 (0.008)	0.012	0.027	0.441 (0.034)
$\hat{\omega}$	0	0.020 (0.004)	0.442 (0.075)	0.055 (0.003)	0.492 (0.010)	0.412	0.214	0.357 (0.019)
$\hat{\omega}_i$				0.205 (0.056)	0.460 (0.020)		0.303	
$\hat{\beta}$	1	1	18.85 (7.715)	1	51.88 (36.69)	25.74	3.458	
LL	-10066.22	-10049.83	-9723.77	-9957.17	-9695.79	-9739.98	-9972.41	-9914.31
BIC	20142	20118	19475	19942	19428	19480	19944	19847
LRT of $\hat{\omega} = 0$ (p-value)		0.000	0.000	0.000	0.000			0.000
i. Posterior Model Prob.	0.000		0.992			0.008		
ii. Posterior Model Prob.	0.000	0.000	0.000	0.000	1.000			0.000

In each of our Divisive Normalization specifications, we find that the estimate of ω is significantly different from zero ($p < 0.001$, LR test). This suggests that we are observing choice behaviour in which the composition of the choice set affects the degree of variance in the model, and therefore the relative choice probabilities. The best performing model unrestricts both ω_i and β , though the point estimate of β is again large and relatively imprecise. As in the trinary experiment, the unrestricted Divisive Normalization models significantly outperform Range Normalization in terms of log-likelihoods and BIC.

The fitted probabilities over the different choice set sizes are reported in Figure 12. The Divisive Normalization model captures the sample choice probabilities for all set sizes, with the slight exception of under-predicting the probability of choosing alternative 3 in large set sizes.²⁴ This is in

²⁴ The increase in the predicted probability of choosing alternative 3 arises from the construction of our choice set. Alternatives 3-12 were randomly sampled from a set of 10 items, which means that smaller choice sets were more likely to have a larger disparity between alternative 3 and the remaining alternatives. The slight under-prediction for large set sizes might result from attentional constraints, or a form of choice set editing, for large choice sets.

contrast to the Range Normalization and Probit models. While Range Normalization is unable to capture the change in probability of choosing the highest alternative as the set size increases, the Probit under-predicts this probability for all set sizes. As a result, for a set size of 12 alternatives, the highest ranked alternative is chosen 5% more often than predicted by a Range Normalization model and the Probit model with a constant variance.²⁵

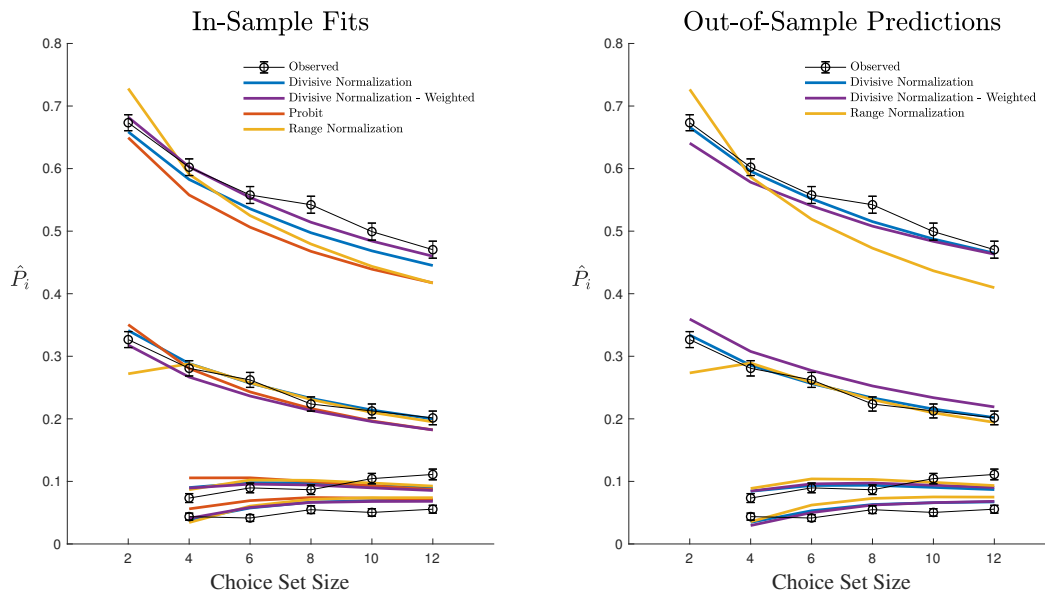


Figure 12 (Left) The fitted probabilities that alternative 1, 2, 3, & 4 are chosen (from top to bottom), over the range of choice set sizes. (Right) The out-of-sample predicted probabilities using the estimates from the trinary experiment.

Finally, we assess the robustness of the Divisive Normalization specification across our two experimental paradigms. Remarkably, the degree of normalization that we observe is largely consistent with the estimates from the same specification of the trinary experiment ($\hat{\sigma}$: 0.001 vs. 0.012; $\hat{\omega}$: 0.442 vs. 0.412; and $\hat{\beta}$: 18.85 vs. 25.74). Restricting the model to the parameter estimates from the trinary experiment yields a slight increase in the log-likelihood (Table 3, second-to-last column), suggesting that the same normalization parameters can capture the relationship between the choice probabilities and the composition of the set across the two experiments. To assess this result, we used the estimated parameters from the trinary experiment to generate predicted choice probabilities for the choice sets in the set size experiment via equation (10). Figure 12 reports these out-of-sample predicted probabilities. We should emphasize that *these are aggregate predictions conducted on a completely separate sample of subjects from a different experimental paradigm.*

²⁵ As noted earlier, interpreting the results from the Probit estimation may be problematic since its estimation is inconsistent in the presence of Divisive Normalization.

Notably, the Divisive Normalization model captures the sample choice probabilities for all set sizes, with the exception of under-predicting the probability of choosing alternative 3 when the set size becomes very large.

4.2.3. Estimation Results and Model Comparison — Modelling Heterogeneity To model heterogeneity in the set size sample, we also considered the random-coefficients specification from (Section 4.1.4), in which the normalization parameter for each subject ω_s is drawn from the Gamma density $g(\omega_s; a, d)$ with shape parameter a and scale d . Results from this analysis are reported in Table 4 and the estimated density of ω_s for both Divisive Normalization and Range Normalization models are depicted in Figure 13.

Table 4 Random coefficient model estimates for the set size choice experiment.

	Divisive Normalization		Range Normalization
\hat{a}	0.839 (0.028)	1.400 (0.274)	0.615 (0.120)
\hat{d}	0.166 (0.123)	0.346 (0.102)	1.128 (0.379)
$\hat{\sigma}$	0.163 (0.040)	0.000 (0.024)	0.283 (0.018)
$\hat{\beta}$	1	4.349 (0.6971)	-
LL	-8971.17	-8759.86	-8933.98
BIC	17951	17528	17877
Posterior Model Prob.	0.000	1.000	0.000

In the case of the Divisive Normalization model, we find that a is significantly different from zero and that the estimated density of ω_s places substantial weight on $\omega_s > 0$ for the specification with β unrestricted. The estimate of β is larger than in the trinary case (4.4349 vs. 2.208), but only marginally significantly so ($p = 0.11$) and still within the range typically observed in sensory systems. The specification which restricts $\beta = 1$, however, is summarily rejected. Similarly, the estimated density for the Range Normalization model places much more weight on $\omega_s = 0$. This model has a smaller log-likelihood and a larger BIC compared to Divisive Normalization with an unrestricted β .

5. Conclusion

In the study of the human brain and behaviour, it has long been recognized that the biology of neural systems is both subject to constraints imposed by finite resources, and shaped by the statistical properties of the environment we live in (Machens et al. 2005, Ganguli and Simoncelli 2014, Wei and Stocker 2017). As a result, the organization and form of neural computation have

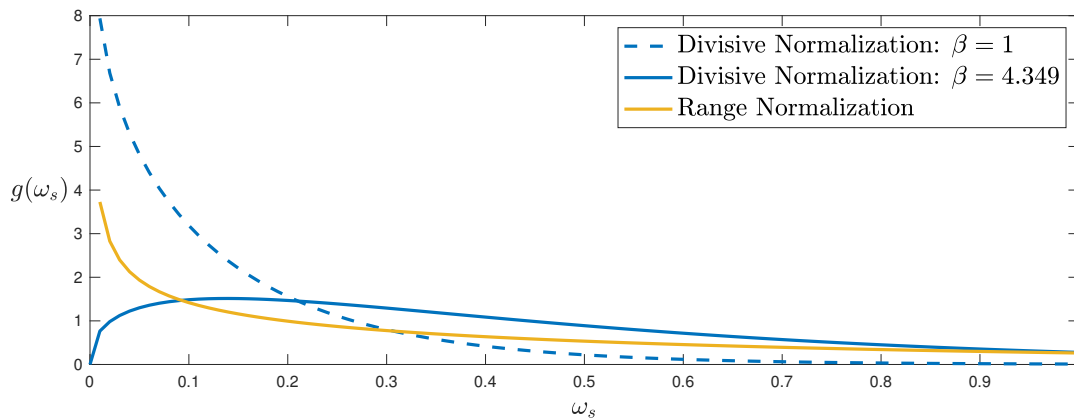


Figure 13 The Probability Density of $\omega_s \sim \text{Gamma}(a, d)$ estimated from the set size experiment.

evolved such that information about the objective world is approximated and/or compressed into quantities that can be encoded in finite, stochastic, neural activity. A growing number of scholars are examining what these constraints imply for choice behaviour, and how behavioural theories can incorporate these insights (e.g. Caplin and Dean 2015, Steiner and Stewart 2016, Hebert and Woodford 2017, Bhui and Gershman 2018, Noguchi and Stewart 2018, Polania et al. 2019).

In this article, we study the role of a canonical neural computation, Divisive Normalization, in shaping valuations during the decision-making process in response to a bound constraint on neural activity. Since Divisive Normalization suppresses, or normalizes, valuations relative to the composition and size of the choice set, it yields predictions about relative choice probabilities that depend on the choice set. The effects of this relationship include increased stochasticity compatible with Weber’s Law, particular patterns of violation of the Independence of Irrelevant Alternatives axiom, and a decreased likelihood of choosing a higher-valued alternative as the composition of the choice set is altered. Notably, we also document robustness in the parameter estimates across paradigms. The structural estimates from an experiment which varies the value of a third alternative are very similar to those in an experiment which varies the size of the choice set, and do a better job of capturing the choice probabilities than a standard Probit and a Range Normalization model fit in-sample. Such robustness in the structural estimates of preference parameters suggests that Divisive Normalization may be a basic property of choice behaviour.

We also address the normative role of the relative valuations induced by the divisive normalization computation. In sensory systems, normalization has been demonstrated to reduce the resources required to encode the statistical properties of our natural environment. However its normative role in decision-making has remained unclear (Louie et al. 2013). The choice behaviour of subjects in our experiments can be strictly deemed inconsistent or perhaps even welfare-decreasing: the highest-ranked alternative was chosen less when both the composition and the size of the choice

set was altered. Why would a neural system – selected over tens of millions of years of evolution – exhibit such adverse choice performance?

We propose that these patterns in choice behaviour provide evidence for a boundedly rational decision-making process under neurobiological constraints. Recall that a neurobiological constraint has two implications: neural activity is both stochastic and bounded. The existence of these constraints re-focuses the normative question. How should the brain encode the valuation of choice alternatives given a neurobiological constraint on the precision and resolution with which it can encode quantities, and why might this encoding scheme follow the form of Divisive Normalization? Our answer is that some degree of normalization is required to compare choice alternatives. Normalization scales valuations to the boundary of this constraint, preserving relative valuations and yielding the fewest possible choice errors. Viewed this way, the adverse choice behaviour we observe is not due to an inefficient or mal-adapted neural architecture, but is in fact an efficient implementation in response to a neurobiological constraint on value representations.

Understanding the mechanism by which the brain encodes relative quantities can be extended into other domains of economic choice behaviour. For instance, choice behaviour in the domain of uncertainty suggests that utilities are determined relative to a reference point (Kahneman and Tversky 1979), perhaps formed as an endogenous expectation over a history (Koszegi and Rabin (2006)). Since the normalization computation scales neural activity relative to the entire choice set, the static model presented here provides a mechanism for how this expectation is formed for the current choice set. A dynamic version of the divisive normalization computation explores implications for behaviour when this expectation is formed over time (LoFaro et al. 2014, Tymula and Glimcher 2016, Zimmermann et al. 2018). More generally, these insights have been extended to the multi-attribute domain. Landry and Webb (2019) extend the normalization computation to address a range of phenomena including well-known *decoy effects* that rely on a particular structure of numerically-presented attributes (Huber et al. 1982, Simonson 1989, Tversky 1972). Related work emphasizes the sequential comparison of attributes relative to a reference sampled from working memory (Noguchi and Stewart 2018).

All together, our results speak to the role of incorporating insights from biology into economic discourse. While developing an understanding of the brain is intriguing in its own right, the goal of neuroeconomic research should be predicting novel patterns in choice behaviour and producing a normative explanation for the behaviour we observe (Bernheim 2009, Glimcher 2011). We argue that incorporating divisive normalization into a choice model accomplishes this goal. Our results emphasize both the positive advances offered by choice models grounded in neuroscience, and the normative role neurobiological constraints can play in the study of choice.

Appendix A: The Neurobiology of Sensation, Valuation, and Choice

Some background on the structure of the brain might be helpful for understanding how decision-making is constrained by neurobiology. The total pool of neurons that make up cortex can be anatomically divided into non-overlapping subsets of neurons, and each of these “areas” is distinct in structure and organization. Empirical evidence suggests that any given area serves a limited set of functional roles – which are the same across individuals – and a small subset of these areas have been identified as having a role in decision-making. It is essentially required by this logic that devoting more neural resources to these decision-making areas must balance the benefits of improved decision-making against the costs of allocation those resources to other functions, such as processing sensory information or managing the heartbeat.

So why is a decision-maker limited in its ability to recruit more neural resources, even if it might be momentarily advantageous? The reason is that brain areas are distinct in their connections with the rest of the brain, distinct in their cellular structure, and distinct in many of their biophysical properties. These specializations, which distinguish different brain areas and make them appropriate for particular functions, develop over years – primarily over the first 20 years of development – and cannot be altered quickly. This imposes a significant constraint on the ability of a decision-maker to endogenously allocate neural resources to a task. For these reasons, we consider the allocation of neural resources to be effectively fixed at a particular moment in time, at least for the time horizon in which decisions are typically made by an individual.²⁶ In this appendix, we will review the literature on the neurobiology of sensation, valuation, and choice in the presence of resource constraints, with particular focus on the Divisive Normalization computation.

A.1. Divisive Normalization in Sensory Systems

A fundamental goal in *systems neuroscience* is to understand how the brain processes and represents information at the level of individual neurons. Much of this work has focused on the sensory domain in which an environmental stimulus is transduced through the sensory organs and passes through a series of processing stages (i.e. spatially and functionally distinct networks of neurons), each of which has a particular role. In the visual system, for instance, photons (which comprise light) make initial contact with photoreceptors in the retina and this information passes through subsequent stages of hierarchical neural processing in retinal ganglion cells, the thalamus, primary visual cortex, and so on. Generally speaking, sensory neurons in these regions are “tuned” for a particular stimulus, for instance the intensity of light in a particular region of visual space, or a particular direction of motion (e.g. Hubel and Wiesel 1968).

At each of these levels, sensory neurons display activity that cannot be solely explained by linear models (the activity of a neuron is not simply a weighted sum of the inputs to that neuron). For instance, neural activity is bounded at high input levels and exhibits the phenomenon of *suppression* — the neural activity elicited by a stimulus (for which the neuron is tuned) is reduced in the presence of a stimulus for which it is

²⁶ There is a large literature in neuroscience and psychology which examines the prevalence of errors as a function of the time spent on a decision, known as the *speed/accuracy tradeoff* (for a review, see Bogacz et al. 2010). This literature finds that one can improve accuracy with longer decision times, but that this increase in accuracy is bounded. The fact that increasing the time devoted to a decision cannot overcome this resource limitation problem reflects a temporal constraint that has been both widely observed and biologically explained, though is not the subject of this article.

not tuned. In the retina, for example, light intensity is encoded relative to the average ambient illumination. This relative representation of information is observed to be a general feature of sensory coding.

The divisive normalization computation was proposed to explain such nonlinear phenomena in primary visual cortex (Heeger 1992). The critical feature of the computation is a divisive rescaling of the activity of a population of neurons by the total activity of a larger pool of neurons. Variations on the form of normalization have appeared in literature, all nested by the general form,

$$f_i(x_1, \dots, x_N) = \kappa \frac{x_i^\alpha}{\sigma + \left(\sum_{n=1}^N \omega_n x_n^\beta\right)^\frac{1}{\gamma}}, \quad (11)$$

where the response $f_i(x_1, \dots, x_N)$ of a population $i \in N$ is a function of both the driving input x_i to that population and the inputs to the other elements of the normalization pool (Lyu and Simoncelli 2008, Lyu 2011, Sinz and Bethge 2013, Ballé et al. 2016a). This general response function is governed by a number of parameters: κ denotes the maximum possible activity level, σ determines how responses saturate with increased driving input, ω_n weights each neural population in the normalization pool, and α , β and γ mediate the form of the normalization.

Divisive Normalization implements several features consistent with how neurons in visual cortex respond to sensory information. First, because the input to a given neuron is also included in the normalization pool, the model produces a saturating response to increases in driving input. This is consistent with the observation that neurons are biologically constrained below a maximum firing rate. Second, division expresses the quantity encoded by a population of neurons in relative terms, scaled to the pooled activity of other inputs. Indeed, divisive normalization appears to be a general feature of information processing in cortical systems (for a review, see Carandini and Heeger 2012). Originally proposed to explain non-linearities in primary visual cortex, normalization has been identified in multiple stages of visual processing from the retina to downstream visual areas, and in species ranging from the fruit fly to primates. In addition to vision, normalization characterizes neural responses in all other sensory modalities, such as audition and olfaction, and extends to higher-order cognitive processes including attention and multi-sensory integration.²⁷

Given the pervasive observation of divisive normalization in sensory systems, the question of its normative role in neural coding has been raised. In systems neuroscience, the benchmark normative framework for information processing is the *efficient coding* hypothesis (Barlow 1961) based on Shannon’s seminal work on information transmission via finite capacity channels. Because neural systems face biological constraints (e.g. maximum firing rates and/or numbers of neurons), the efficient coding hypothesis holds that sensory stimuli should be represented in a manner that minimizes the redundancy in encoded information; that is, neural responses should be statistically independent. Crucially, the statistics of the natural environment are

²⁷ We should note that the normalization model describes a computational algorithm rather than a specific biophysical implementation. Researchers have identified a number of potential neural mechanisms for implementing normalization and it is likely that the normalization computation is mediated by different processes in different species and systems. Moreover, since evolution selects on the fitness of the output of a particular neural system, the parametrization of the normalization equation will depend on the role of the particular system and statistical features of its input. The widespread occurrence and varying implementations indicate that it is the normalization computation, rather than the specific mechanism and/or parameterization, which is critical to efficient neural systems.

decidedly not independent. For instance, regions of visual space with intense light occur in clusters, unlike the statistically independent “snow” displayed on an un-tuned analog television set. Under the efficient coding hypothesis, sensory systems should transform information about the natural world into a less redundant representation by incorporating these dependencies directly in coding algorithms.

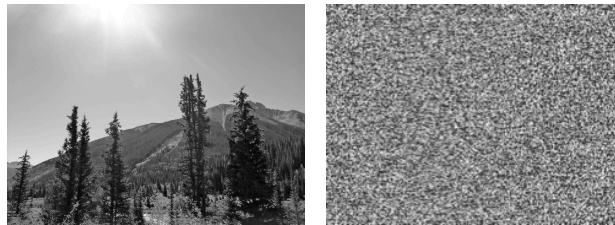


Figure 14 In the natural environment, nearby regions of visual space tend to be correlated (left), not independent (right). When correlated, information on one region can be used to predict information in another, therefore it is redundant.

While linear weighting functions can remove some redundancies, the statistics of natural images are too complex for linear models to produce completely independent responses. By contrast, the non-linear divisive normalization model markedly reduces higher-order correlations in responses to both natural images and sounds (Schwartz and Simoncelli 2001, Lyu 2011, Sinz and Bethge 2013, Ballé et al. 2016a), and has been shown to implement near-optimal categorization and encoding of these sensory stimuli (Qamar et al. 2013). Thus there is compelling evidence that normalization serves a specific normative role in implementing efficient information coding in sensory systems.

However, this constrained encoding scheme (like all constrained optimal solutions) has consequences. While the encoding itself is efficient given the constraint, it can still lead to errors in perception, and ultimately, choice. Consider the image known as the “Checkerboard Illusion” depicted in Figure 15. If required to decide which of the two regions “A” and “B” appears brighter, one could not be faulted for choosing B. In fact, the luminance of the two regions is precisely the same. However B *appears* brighter due to the normalization computation performed at the level of the retina and visual cortex. The luminance of region B is encoded relative to nearby locations that fall in a shadow, and is therefore normalized to a lesser extent than A. Therefore B appears brighter even though it is of the same (objective) luminance, potentially resulting in a choice error.

A.2. Divisive Normalization of Valuations

The ubiquity of divisive normalization in sensory brain areas, and the general similarity of information processing in neural systems, suggests that a form of normalization may also be taking place in regions of cerebral cortex that are involved in decision-making. Recent neural evidence from primates supports this contention (Rorie et al. 2010, Louie et al. 2011, Pastor-Bernier and Cisek 2011). For example, Louie et al. (2011) examined the activity of neurons in the LIP area of the monkey brain. The activity of individual LIP neurons varies with the quantity of the reward associated and is involved in the selection of actions (see

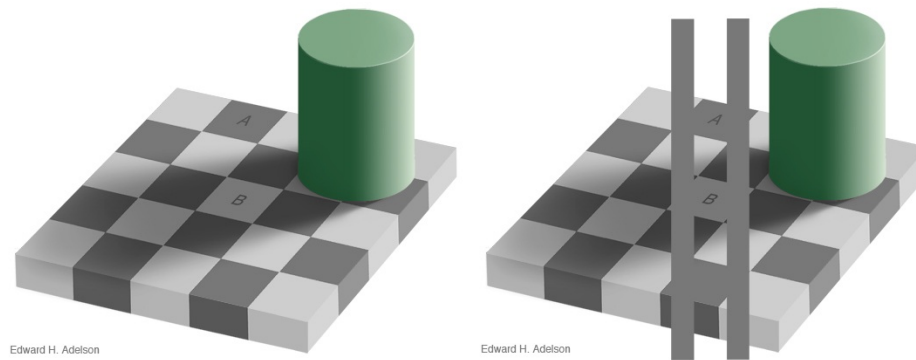


Figure 15 The “Checkerboard Illusion.” Regions “A” and “B” have equal luminance. [Source] Reproduced with permission from <http://persci.mit.edu/gallery>.

Appendix A.3.2). In the Louie et al. (2011) experiment, multiple alternatives were displayed on a screen, and the value of one alternative (in ml of water) was held constant while the number and value of the other alternatives were varied. In the absence of normalization, varying the other alternatives should elicit no change in activity from the neuron which encoded for the constant target. Nonetheless, the measured neural activity varied inversely with the number and value of the alternatives, consistent with a model in which the neural activity coding the value of a specific alternative is suppressed by the value of others (see Figure 16). Furthermore, a simple Divisive Normalization model provides a stronger account of this neural data than other candidate explanations, suggesting a common form of information coding in sensory and decision-related neural activity. Such relative value coding is likely to be a common feature of action-selective decision areas, empirically demonstrated in parietal cortex (Louie et al. 2011, Rorie et al. 2010), dorsal premotor cortex (Pastor-Bernier and Cisek 2011), striatum (Klein et al. 2017, Wang et al. 2013), and the superior colliculus (Basso and Wurtz 1997). Reviews of this literature can be found in Seymour and McClure (2008), Rangel and Clithero (2012), Louie et al. (2015).

A.3. A Two-Stage Model of Valuation and Choice

To examine the role of Divisive Normalization in shaping valuations during choice, we focus on a basic two-stage decision model in the primate brain. This model is predicated on a distinction between brain regions that aggregate value information from attributes in an action-independent manner and those that employ that value information in the process of choice (Platt and Plassmann 2013, Polania et al. 2015). In Figure 17, we provide a conceptual description of this model. We should emphasize that our focus on the simple two-stage formulation of valuations and choice is to highlight the role normalization plays in shaping valuations as they transition between between frontal and parietal regions of the brain during decision-making, not because the two-stage model is the focus of our exposition. This model can be expanded to allow for multiple stages of processing with interaction between these stages (e.g. Cisek 2012, Platt and Plassmann 2013, Cai and Padoa-Schioppa 2014, Hunt and Hayden 2017). Indeed, a recent perspective proposes that information transitions through multiple levels of processing with a computation akin to Divisive Normalization at each of these levels (Yoo and Hayden 2018). This flow of information can arise indirectly through other cortical or

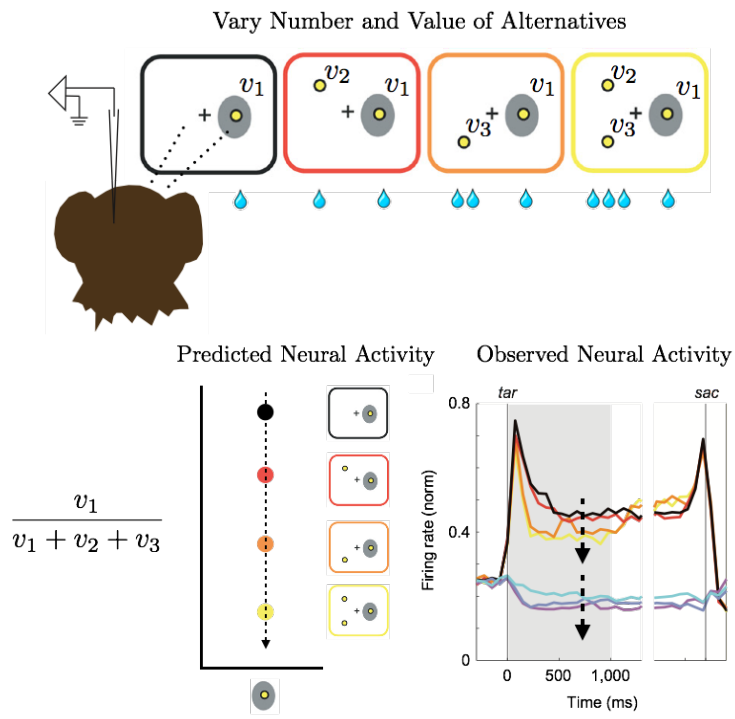


Figure 16 The Louie et al. (2011) experiment in which a monkey is evaluating choice alternatives. Neural activity is recorded for a constant alternative v_1 (grey circle), while the number and value (in μl of water) of the other alternatives is varied. The average activity (firing rate) of the recorded neurons over the course of the trial is reported.

sub-cortical structures, therefore does not require direct connectivity between cortical regions (Moisa et al. 2018).

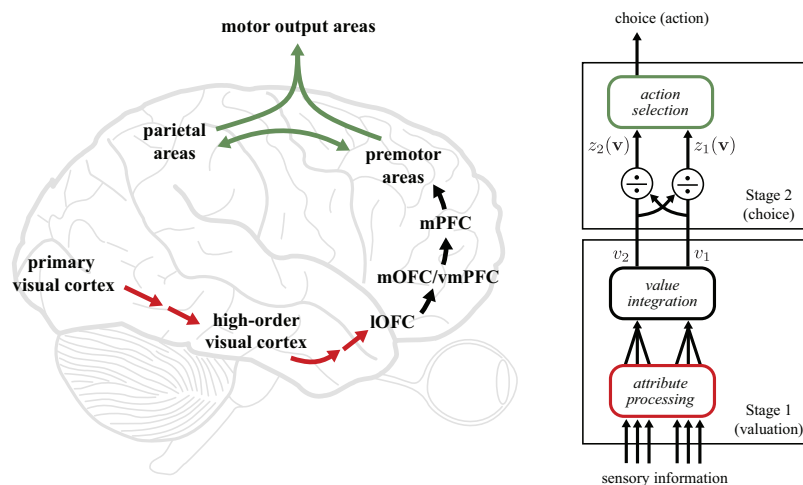


Figure 17 Conceptual Model of Two-Stage Decision Process in the Human Brain. The coloured arrows (left) reflect the temporal flow of information through these stages (right), rather than direct connectivity. Sub-cortical pathways are not depicted.

A.3.1. The First Stage - Value Integration The representation of an integrated value signal in frontal brain regions is supported by multiple lines of evidence, including anatomical connectivity, neural activity recordings, and lesion studies. Consistent with a region performing integrative valuation, anatomical studies document that frontal brain regions receive sensory inputs from visual, auditory, gustatory, olfactory, and somatosensory systems along with memory systems in perirhinal cortex and hippocampus (Ongür and Price 2000, Camara et al. 2009, Shadlen and Shohamy 2016).²⁸ Neurophysiological and neuroimaging studies further support the hypothesis that frontal areas are involved in the integration of value information. Over 200 studies have demonstrated that activity in these brain regions is correlated both with the valuations that humans place on different items, as well as information about the individual attributes from which those values are derived (Bartra et al. 2013, Levy and Glimcher 2012, Clithero and Rangel 2013, for reviews).²⁹

Consistent with a representation of integrated value (a neural “common currency”), frontal brain regions encode multiple aspects of individual rewards such as magnitude, probability, and sensory features (Tremblay and Schultz 1999, Kennerley and Wallis 2009, Rich and Wallis 2016) and correlate with the willingness-to-pay of a range of different objects such as food, consumer items, lotteries, and social rewards (Plassmann et al. 2007, Chib et al. 2009, FitzGerald et al. 2009, Lin et al. 2012). Importantly, information about specific attributes or good categories is most distinguishable in lateral and ventral regions of orbito-frontal cortex (Hare et al. 2011a, McNamee et al. 2013, Suzuki et al. 2017), suggesting that attribute-level information is integrated into a neural representation of value as it transitions towards medial pre-frontal areas. It is these latter regions which can be used to measure valuations of consumer items in the absence of choice behaviour (Levy and Glimcher 2011, Smith et al. 2014), and have been shown to correlate with the willingness-to-pay measured from bidding procedures on consumer goods (Plassmann et al. 2007, Chib et al. 2009).³⁰ In our model, these valuations are denoted $\mathbf{v} = [v_1, \dots, v_N]$ for the alternatives $\{1, \dots, N\}$ and are measured directly using a willingness-to-pay procedure.

A.3.2. The Second Stage - Action Selection In the second stage of neurobiological decision-making, subjective (or constructed) value information is utilized by neural circuits that implement a decision. The predominant model for this choice process is based on models of perceptual decision-making (Gold and Shadlen 2007, Cisek and Kalaska 2010, Summerfield and Tsetsos 2012, Shadlen and Kiani 2013), in which decisions are physically implemented as arm reaches or eye movements, and neural activity is examined in

²⁸ In particular, frontal brain regions receive prominent projections from the amygdala and posterior granular orbital insula (Porrino et al. 1981, Carmichael and Price 1996), brain regions involved in processing reward information and olfactory, gustatory and visceral sensory information respectively. Frontal brain regions also send projections to the ventral striatum, one of the core brain regions identified in functional neuro-imaging studies as representing the subjective valuation of choice alternatives (Bartra et al. 2013).

²⁹ This evidence extends beyond human fMRI to direct observation of neural activity via electrophysiological recording. Neurons in the monkey orbitofrontal cortex represent the economic value of options at the time of decision making (Padoa-Schioppa and Assad 2006, Padoa-Schioppa and Conen 2017)

³⁰ In addition, lesion studies in both monkeys (Rudebeck et al. 2017, Izquierdo 2004) and humans (Noonan et al. 2017, Camille et al. 2011) demonstrate that frontal brain regions are necessary for value-guided choice behaviour.

the relevant brain structures.³¹ These brain structures typically receive both bottom-up sensory information and top-down information from frontal brain regions, perhaps indirectly through cortical and sub-cortical structures like striatum (Polania et al. 2015, Moisa et al. 2018), and are closely related to movement-related circuits.³² Critically, activity in these brain regions also covary with the values of the rewards associated with those particular actions, suggesting that this *action value* information is incorporated into the dynamic processes that determine choice. However, in contrast to first-stage brain regions, neural activity in second-stage areas represent the value of actions regardless of the specific attributes that might contribute to value, and typically do not represent isolated attributes.

For example, when choices are made via eye-movements (a saccade toward a selected alternative), the activity of saccade-selective neurons covaries with the value associated with the target. Such action values have been identified in numerous decision-related oculomotor structures including the lateral intra-parietal area (LIP) (Platt and Glimcher 1999, Sugrue et al. 2004).³³ The activity of LIP neurons correlates with the subjective value of potential saccades, whether this value is determined by sensory contingencies, reward magnitude and probability, delay discounting, foraging requirements, social information, or strategic valuation in a competitive game.³⁴ Thus, action-selective neurons — that typically project directly or indirectly to the circuits that implement a particular choice — encode the integrated subjective values of their associated actions. A number of recent fMRI studies, performed with human subjects implementing choices on a keyboard, also suggest that value signals from medial pre-frontal regions are accumulated and compared during the choice process in dorso-lateral cortex and the intra-parietal sulcus (Basten et al. 2010, Hare et al. 2011b, Domenech et al. 2017). Formally, this process can be modelled by appending a stochastic error term $\boldsymbol{\eta} = [\eta_1, \dots, \eta_N] \in \mathbb{R}^N$ to valuations constructed in the first stage as in Equation (3) (Webb 2019).

A.3.3. Summary We are guided to this formulation of a choice model by two key observations from the neurobiological literature. First, both human-imaging and electrophysiological evidence is consistent with binary choice decisions being implemented via a stochastic, dynamic, accumulation of value information in dorso-lateral and parietal cortex. Second, the electrophysiological evidence for divisive normalization in valuation tasks has been observed in the *same* brain regions, suggesting the divisive normalization computation is implemented prior to, or in conjunction with, this second-stage accumulation. Our aim is to model the

³¹ In primate experiments, neural activity in orbito-frontal cortex also correlate with value and choice information. This has led to the hypothesis that decisions can also occur in an action-independent framework, with choices made between options independent of the particular motor action used to implement choice (Padoa-Schioppa 2011, Cai and Padoa-Schioppa 2014), or perhaps in conjunction with action-selective regions (Cisek 2012, Padoa-Schioppa and Conen 2017). Our model of value normalization is consistent with either interpretation, it simply requires a hypothesis about the brain region in which the normalization computation is operating. The same model would describe goods-based choice as long as the neurons which actually implement a selection process receive normalized inputs. The critical hypothesis is that normalization takes place over options regardless of whether the values are coded in an action-dependent or -independent framework.

³² In particular, decision-related activity has been identified in high-level sensory association areas in parietal cortex, premotor cortical brain regions, and subcortical structures such as the striatum and superior colliculus.

³³ Similar results have been observed in the frontal eye fields (Ding and Hikosaka 2006), the superior colliculus (Ikeda and Hikosaka 2003), and the caudate nucleus in the striatum (Samejima 2005)

³⁴ Shadlen and Newsome (2001), Roitman and Shadlen (2002), Louie and Glimcher (2010), Platt and Glimcher (1999), Dorris and Glimcher (2004), Klein et al. (2008), Sugrue et al. (2004)

transformation of valuations in this second stage. We therefore interpret \mathbf{v} as a decision maker's independent valuation of a consumer good, however constructed, and study the choice behaviour implied when these valuations are normalized in the implementation of a decision via $z(\mathbf{v})$ and the stochastic process captured by $\boldsymbol{\eta}$.

Again, we strongly suspect that the brain implements relative coding in earlier stages of the decision-making process — for instance in the construction of \mathbf{v} from objective sensory attributes, perhaps in regions of orbito- and pre-frontal cortex. Electrophysiological evidence for adaptive coding in orbito-frontal regions can be found in Padoa-Schioppa (2009). Chau et al. (2014) provide some initial fMRI evidence, though see Gluth et al. (2016). At the behavioural level, Landry and Webb (2019) and Noguchi and Stewart (2018) provide reviews of the modelling literature in Economics and Psychology which implement relative coding at the level of attributes. The interaction of relative coding at multiple stages of the decision-making process, and how these representations interact to shape the form of context-dependent preferences, remains an exciting area for further research.

Appendix B: Closed Form Results for Divisive Normalization

We now explore some formal properties of the Divisive Normalization model when the error density is given by the Gumbel distribution. The tractability of this distribution yields clear theoretical results for violations of regularity and membership in the class of set-dependent Luce models (Marley et al. 2008).

B.1. Divisive Normalization and Regularity

First, we find that Divisive Normalization will technically violate the regularity condition for some, but not all, values and parameterizations of the model. Our proof focuses on the Gumbel distribution since it has closed-form probabilities. We have not yet characterized the entire range of distributions and range of valuations for which regularity fails, but extensive simulation suggests it is small.

We begin with a definition of Random Utility. Let $P_{i,N}$ denote the probability that a subject chooses alternative i from a finite set N .

DEFINITION 1. (Random Utilities) There exists a random vector $U=(U_1, \dots, U_n)$, unique up to an increasing monotone transformation such that for any $i \in M \subseteq N$,

$$Pr\{U_i \geq U_j, \forall j \in M\} = P_{i,M}.$$

A necessary condition for a random utility representation states that the probability of choosing an alternative decreases as more alternatives are added to the choice set (Block and Marschak 1959), often referred to as a *regularity condition*.

DEFINITION 2. (Regularity) If $L \subseteq M \subseteq N$,

$$P_{i,M} \leq P_{i,L}.$$

We now show that a model with normalization violates the regularity condition for some parameter values, therefore cannot be rationalized by a Random Utility model. We consider two choice sets of different sizes, the three alternative choice set $\{1,2,3\}$, with corresponding valuations $v_1 \geq v_2 \geq v_3 \geq 0$, and the two alternative subset $\{1,2\}$. Since we are assuming a Gumbel distribution, the choice probabilities of the normalized model are given by the closed form equation,

$$P_{i,M} = \frac{e^{\frac{v_i}{\omega \sum_{n \in M} v_n}}}{\sum_{m \in M} e^{\frac{v_m}{\omega \sum_{n \in M} v_n}}}. \quad (12)$$

We will focus on the probability of choosing the second (ranked) alternative from the set. For our simple choice sets, these probabilities can be re-written

$$P_{2,\{1,2,3\}} = \frac{1}{e^{\frac{v_1-v_2}{\omega(v_1+v_2+v_3)}} + e^{\frac{v_3-v_2}{\omega(v_1+v_2+v_3)}} + 1},$$

and

$$P_{2,\{1,2\}} = \frac{1}{e^{\frac{v_1-v_2}{\omega(v_1+v_2)}} + 1}.$$

We will show regularity is violated as the choice set is expanded from two to three alternatives.

PROPOSITION 4. *There exists some $\bar{\omega} > \omega \geq 0$ such that the choice probabilities:*

1. are Regular for all $\omega > \bar{\omega}$, therefore can be represented by Random Utilities.
2. are not Regular for all $\omega < \bar{\omega}$, therefore cannot be represented by Random Utilities.

Proof Part 1. requires that there is some $\bar{\omega} \geq 0$ such that $P_{2,\{1,2,3\}} < P_{2,\{1,2\}}$ if $\omega > \bar{\omega}$. Note that $P_{2,\{1,2,3\}} < P_{2,\{1,2\}}$ if and only if

$$\begin{aligned} e^{\frac{v_1-v_2}{\omega(v_1+v_2+v_3)}} + e^{\frac{v_3-v_2}{\omega(v_1+v_2+v_3)}} + 1 &> e^{\frac{v_1-v_2}{\omega(v_1+v_2)}} + 1 \\ e^{\frac{v_1-v_2}{\omega(v_1+v_2+v_3)} - \frac{v_1-v_2}{\omega(v_1+v_2)}} + e^{\frac{v_3-v_2}{\omega(v_1+v_2+v_3)} - \frac{v_1-v_2}{\omega(v_1+v_2)}} &> 1 \\ e^{-\frac{(v_1-v_2)v_3}{\omega(v_1+v_2)(v_1+v_2+v_3)}} + e^{-\frac{v_1^2+v_1v_2-2v_2v_3}{\omega(v_1+v_2)(v_1+v_2+v_3)}} &> 1. \end{aligned}$$

Since $v_1^2 + v_1v_2 - 2v_2v_3 > 2v_1v_3 - 2v_2v_3 > (v_1 - v_2)v_3 \geq 0$, the above expression is true if $e^{-\frac{v_1^2+v_1v_2-2v_2v_3}{\omega(v_1+v_2)(v_1+v_2+v_3)}} > \frac{1}{2}$, or equivalently,

$$\omega > \frac{1}{-\log(\frac{1}{2})} \left(\frac{v_1^2 + v_1v_2 - 2v_2v_3}{(v_1 + v_2)(v_1 + v_2 + v_3)} \right) > 0.$$

Part 2. requires that there is some $\bar{\omega} \geq 0$ such that $P_{2,\{1,2,3\}} < P_{2,\{1,2\}}$ if $\omega < \bar{\omega}$. Reversing the inequality (and argument) from above, $P_{2,\{1,2,3\}} < P_{2,\{1,2\}}$ if $e^{-\frac{(v_1-v_2)v_3}{\omega(v_1+v_2)(v_1+v_2+v_3)}} < \frac{1}{2}$, or equivalently,

$$\omega < \frac{1}{-\log(\frac{1}{2})} \left(\frac{(v_1 - v_2)v_3}{(v_1 + v_2)(v_1 + v_2 + v_3)} \right) > 0.$$

□

Note that this result has an important qualification, namely regularity violations are only present for certain values of ω . This means that, for a subject with a given ω , there are only certain subsets of choice sets in which we should expect to see regularity violations. In particular, these violations will be more likely when v_3 and ω are both small.

B.2. Divisive Normalization and Set-Dependent Luce Models

Marley et al. (2008) introduced a class of *set-dependant Luce Models*, in which choice can be represented by a positive scale $b(i)$ and a positive scale $\phi(M)$ on choice sets $M \subseteq N$, where

$$P_{i,M} = \frac{b(i)\phi(M)}{\sum_n b(n)\phi(M)}.$$

In particular, such a representation holds if the choice probabilities satisfy two conditions. The first, originally described by Marley et al. (2008), requires that the choice ratios for any two alternatives vary over sets by a constant ratio.

DEFINITION 3. Set-Dependent Constant Ratio Rule

$$\frac{\log \frac{P_{i,L}}{P_{j,L}}}{\log \frac{P_{i,M}}{P_{j,M}}} = \frac{\log \frac{P_{k,L}}{P_{l,L}}}{\log \frac{P_{k,M}}{P_{l,M}}}, \quad (13)$$

for all $i, j, k, l \in L \cap M$ where $L \subseteq N$, and $M \subseteq N$.

The second necessary condition imposes monotonicity on the choice probabilities, as noted by Stevenson et al. (2018):

DEFINITION 4. Ordering

$$P_{i,L} > P_{j,L} \text{ if and only if } P_{i,M} > P_{j,M}, \quad (14)$$

for all $i, j \in L \cap M$ where $L \subseteq N$, and $M \subseteq N$.

It is straightforward to show that a Divisive Normalization model (with Gumbel errors) satisfies both conditions. Working from equation (12), Divisive Normalization maintains ordering in the choice probabilities since $P_{i,M} > P_{j,M}$ if and only if $v_i > v_j$ iff and only if $P_{i,L} > P_{j,L}$. Moreover,

$$\log \frac{P_{i,L}}{P_{j,L}} = \frac{v_i - v_j}{\omega \sum_{n \in L} v_n}.$$

Therefore condition (13) reduces to $\frac{\omega \sum_{n \in M} v_n}{\omega \sum_{n \in L} v_n} = \frac{\omega \sum_{n \in M} v_n}{\omega \sum_{n \in L} v_n}$, thus is independent of the particular alternatives.

Appendix C: Within-Subject Estimation Results of Trinary Experiment

The normalization model can also be analyzed at the level of each subject to gauge heterogeneity in context-dependent choice behaviour. For example, when a subject faces a choice set in which the value of alternative 3 is large, we should expect to see a smaller ratio of alternative 1 chosen relative to alternative 2. A simple median split of the choice sets (per subject) confirms this intuition. The ratio $\frac{\hat{P}_1}{\hat{P}_2}$ is smaller for the upper median of b_3 for 34 of 40 subjects, with 13 of them significantly smaller at the 0.05 level.

Divisive Normalization also yields a prediction about *how much* context-dependent choice behaviour we should observe for a given range of choice sets. If v_1 and v_2 are far apart, or if v_3 varies by a lot we should expect the choice effects of divisive normalization to be strong. In contrast, if v_1 and v_2 tend to be close together, or if v_3 does not vary by much, then we should expect them to be weak. Therefore heterogeneity in the distribution of valuations that each subject placed on individual items can be used as an additional test of the model.

We assessed this prediction with two methods. Figure 18 reports the maximum likelihood point estimates of the normalization model (7) for each subject. We report the estimate $\hat{\omega}$ multiplied by the average value of the choice set to give a sense of scale relative to $\hat{\sigma}$.³⁵ There is strong evidence for normalization in over half of the subject sample (21/40 subjects at the 0.10 level, 17/40 subjects at a 0.05 level). However heterogeneity in the sample is clearly present in these subject-level point estimates, with the model assigning variance to either σ (red) or to the normalization term governed by ω (blue).

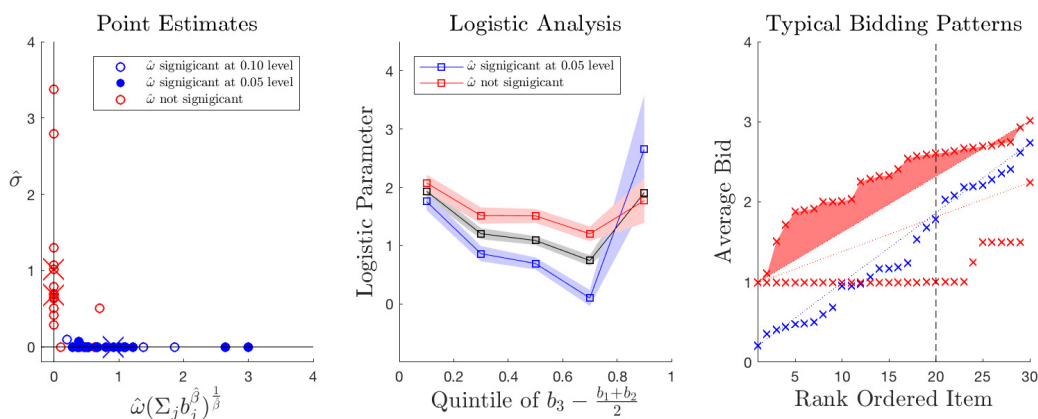


Figure 18 (Left) The point estimates of σ vs. ω for each subject. (Middle) A logistic analysis re-estimated for sub-samples of subjects. The pooled analysis from Section 4.1.2 is reported in black. (Right) The range of bids for the set of items (shown for the 3 subjects denoted with an ‘x’ in the left panel). The red polyhedron depicts the departure of the observed bids (for one subject) from a line between the minimum and maximum bid.

To assess this degree of heterogeneity, we conducted a hierarchical Bayesian analysis which assigns a probability to each subject belonging to one of two clusters. For each cluster $c \in 1, 2$, the normalization parameters (σ , ω , and β) are each drawn from a Gamma distribution with hyper-parameters a_c and d_c (scale

³⁵ The statistical significance of the estimate $\hat{\omega}$ is calculated via a likelihood ratio test from the restricted model with $\omega = 0$.

and shape, respectively).³⁶ The posterior density of the normalization parameters, for each subject, reflects the probability that the subject belongs to each of these clusters multiplied by the Gamma density for each cluster, thus how likely a given parameter value generated the data. Figure 19 reports the posterior density for ω for each of the subjects. Out of the 40 subjects in the sample, we find that the posteriors place more weight on $\omega > 0.05$ than on $\omega < 0.05$ for 28 of the 40 subjects (in blue). Moreover, these are also the same subjects identified via the subject-specific point estimates ($\text{corr}=0.47, p < 0.002$). Notably, the differences between the clusters arise primarily in the hyper-parameter densities for ω , suggesting that the model is separating the clusters based on the degree of normalization evident in the choice probabilities (Figure 20).

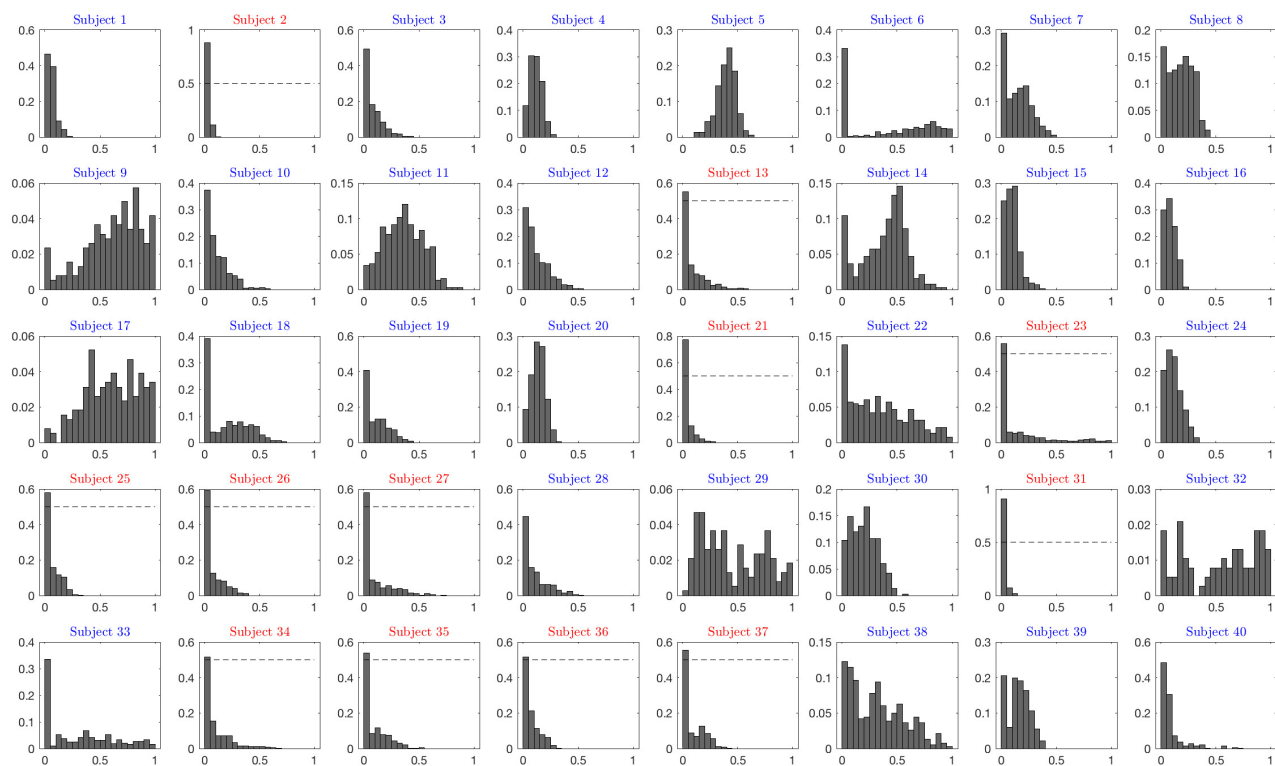


Figure 19 The posterior density of $\hat{\omega}$, for each subject, estimated via a hierarchical Bayesian analysis. The posteriors for subjects coded in blue place more density on $\hat{\omega} > 0.05$ and red place more density on $\hat{\omega} < 0.05$.

The implications of this heterogeneity in the choice probabilities can be visualized if we repeat the logistic analysis from Louie et al. (2013) on sub-samples of subjects for which the point estimates $\hat{\omega}$ are significant or not (Figure 18.B). The subset of subjects which yield a significant $\hat{\omega}$ exhibit a strong contextual effect

³⁶ We conducted analyses with both a uniform prior, and a prior which places substantial density on $\omega = 0$. Results were similar in both cases, suggesting that the prior has limited effect on the results (we report results for the “uninformative” prior). The uninformative prior has the benefit of allowing the posterior to be interpreted as the likelihood, thus providing a conceptual link to frequentist analysis.

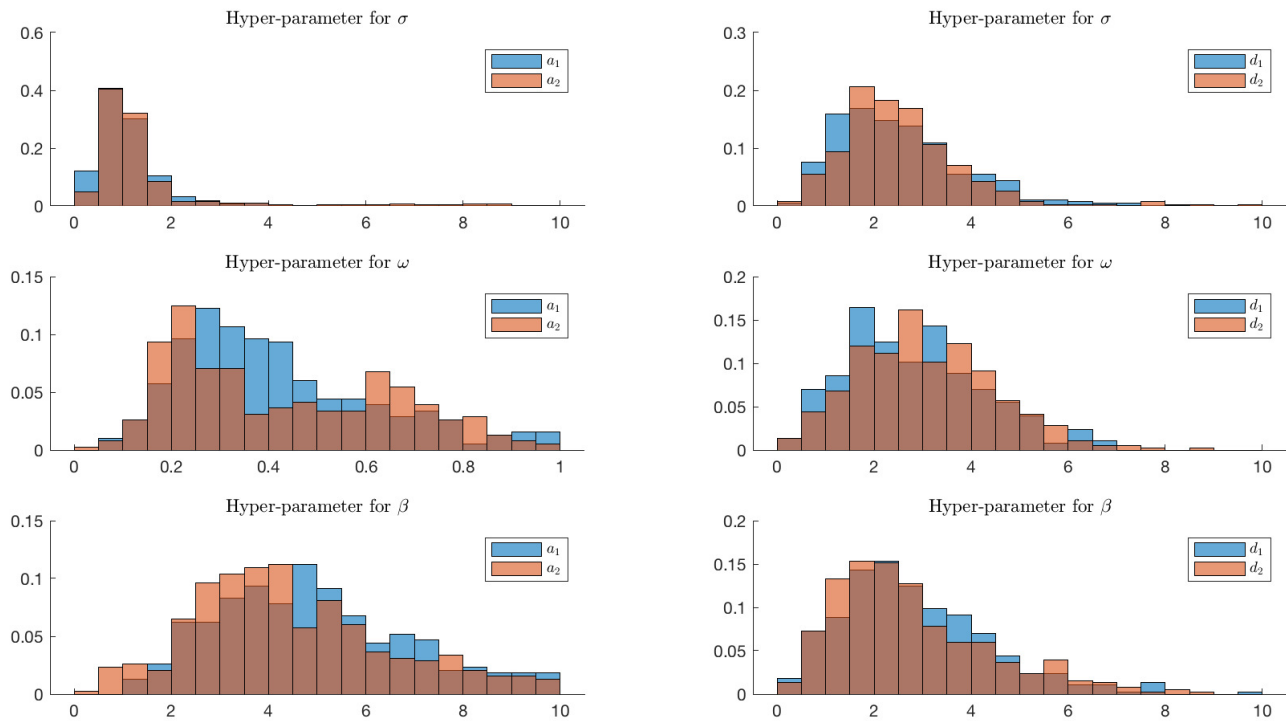


Figure 20 The posterior densities for two clusters of the hyper-parameters (left: scale, right: shape) for the Gamma Distributions of σ , ω , and β .

on the choice probabilities, in contrast to the remaining subjects in which the effect on choice probabilities is much weaker. Results are similar both if we split the sample at the 0.10 level and if we split it by the threshold on posterior densities identified by the hierarchical analysis in Figure 19.

How might this heterogeneity in substitution patterns relate to the underlying bids? In Figure 18.C we highlight the ordered bids of three subjects, two of which with estimates of $\hat{\omega} \approx 0$ (in red). One of these subjects has a small range of bids for alternative 3 (b_3), while the other has a small range of bids for alternative 1 & 2 (b_1, b_2), relative to the subject with $\hat{\omega} > 0$ (in blue). Note that the bid spectrum of this latter subject has roughly equal range for both distractors and targets, therefore is roughly linear compared to the subjects with small $\hat{\omega}$.

To test this possible explanation for the heterogeneity we observe in our subject sample, we constructed a measurement of how much variation is present in valuations of the item set. For each item, we calculated the square of the difference between the rank-ordered valuations and a line which ranges from the minimum bid to the maximum bid. A subject for which the target and distractor set shared a similar range would exhibit a small measurement of variation and a large amount of normalization. A subject for which either the low-value items or high-value items yielded differing ranges of valuations would exhibit a large measurement and little normalization. We then averaged this metric over the two subsets of subjects defined by our regression results, and found it was significantly larger ($p = 0.041$, two-sample t-test, two-tailed) for those

subjects which did not exhibit normalization. This suggests that the small estimates of $\hat{\omega}$ we observed for some subjects resulted from a set of choice alternatives which were not conducive to generating choice set effects (for those subjects). Put another way, Divisive Normalization predicts that we should not expect to see choice set effects in those subjects.

Appendix D: Consumer Goods Used in Experiment



Figure 21 Two examples of item images presented to the subject during the experiment.

Table 5 List of Snackfood Items Presented to Subjects

Almond Joy candy bar	Haribo Gold-Bears gummi candy	Raisinets chocolate raisins
Cashews (whole salted)	Jelly Belly jelly beans	Reese's Peanut Butter Cups
Cheez-It baked snack crackers	Juicyfruits candy	Ritter Sport chocolate bar
Combos baked snacks	Kit Kat Extra Crispy candy bar	Ruffles potato chips
Cracker Jack (caramel popcorn)	Lay's Barbecue potato chips	Smartfood popcorn (white cheddar)
Doritos tortilla chips (cool ranch)	Milk Duds (chocolate and caramel)	Snickers candy bar
Duke's beef jerky (teriyaki flavor)	M&M's chocolate candy	Sour Patch Kids candy
Frito's corn chips	Oreo cookies	Swedish Fish candy
Goldfish baked snack crackers	Planter's Peanut Bar candy bar	Toblerone chocolate bar
Goobers chocolate coated peanuts	Pringles potato crisps	Twizzlers candy

Acknowledgments

The authors wish to thank A. Caplin, N.G. Martineau, T. Strzalecki, K. Train, and T. LoFaro for helpful comments, as well as seminar participants at Harvard University, the University of Zurich, Maastricht University, Princeton University, Northwestern University, and the Ohio State University. We also thank M. Bukwich, M. Khaw, and R. Daviet for excellent research assistance. This research was funded by the Army Research Office (W911ND-11-1-0482), and the experiments were approved by an ethics review panel at NYU.

References

- Alonso R, Brocas I, Carrillo JD (2014) Resource Allocation in the Brain. *The Review of Economic Studies* 81(2):501–534.
- Ballé J, Laparra V, Simoncelli EP (2016a) Density Modeling of Images using a Generalized Normalization Transformation. *ICLR*.
- Ballé J, Laparra V, Simoncelli EP (2016b) End-to-end Optimized Image Compression. *ICLR*, 123–151.
- Barlow HB (1961) Possible principles underlying the transformation of sensory messages. Rosenblith WA, ed., *Sensory Communication* (MIT Press).
- Bartra O, McGuire JT, Kable JW (2013) The valuation system: a coordinate-based meta-analysis of BOLD fMRI experiments examining neural correlates of subjective value. *NeuroImage* 76:412–427.
- Basso MA, Wurtz RH (1997) Modulation of neuronal activity by target uncertainty. *Nature* 389(6646):66–69.
- Basten U, Biele G, Heekeren HR, Fiebach CJ (2010) How the brain integrates costs and benefits during decision making. *Proceedings of the National Academy of Sciences* 107(50):21767–21772.
- Becker GM, DeGroot MH, Marschak J (1964) Measuring utility by a single-response sequential method. *Behavioral Science* 9(3):226–232.
- Bernheim BD (2009) On the potential of neuroeconomics: a critical (but hopeful) appraisal. *American Economic Journal: Microeconomics* 1(2):1–41.
- Bhatia S, Stewart N (2018) Naturalistic multiattribute choice. *Cognition* 179:71–88.
- Bhui R, Gershman S (2018) Decision by sampling implements efficient coding of psychoeconomic functions. *Psychological Review* .
- Block HD, Marschak J (1959) Random Orderings and Stochastic Theories of Responses. *Cowles Foundation Discussion Papers* .
- Bogacz R, Wagenmakers EJ, Forstmann BU, Nieuwenhuis S (2010) The neural basis of the speed-accuracy tradeoff. *Trends in neurosciences* 33(1):10–16.
- Bushong B, Rabin M, Schwartzstein J (2016) A Model of Relative Thinking .
- Cai X, Padoa-Schioppa C (2014) Contributions of orbitofrontal and lateral prefrontal cortices to economic choice and the good-to-action transformation. *Neuron* 81:1140–1151.

- Camara E, Rodriguez-Fornells A, Ye Z, Münte TF (2009) Reward networks in the brain as captured by connectivity measures. *Frontiers in Neuroscience* 3(3):350–362.
- Camille N, Griffiths CA, Vo K, Fellows LK, Kable JW (2011) Ventromedial frontal lobe damage disrupts value maximization in humans. *The Journal of Neuroscience* 31(20):7257–7532.
- Caplin A, Dean M (2015) Revealed preference, rational inattention, and costly information acquisition. *The American Economic Review* 105(7):2183–2203.
- Carandini M, Heeger DJ (2012) Normalization as a canonical neural computation. *Nature Reviews Neuroscience* 13(1):51–62.
- Carandini M, Heeger DJ, Movshon JA (1997) Linearity and Normalization in Simple Cells of the Macaque Primary Visual Cortex. *The Journal of Neuroscience* 17(21):8621–8644.
- Carmichael ST, Price JL (1996) Connectional networks within the orbital and medial prefrontal cortex of macaque monkeys. *Journal of Comparative Neurology* 371(2):179–207.
- Chau BKH, Kolling N, Hunt LT, Walton ME, Rushworth MFS (2014) A neural mechanism underlying failure of optimal choice with multiple alternatives. *Nature Neuroscience* 17(3):463–470.
- Chib VS, Rangel A, Shimojo S, O’Doherty JP (2009) Evidence for a common representation of decision values for dissimilar goods in human ventromedial prefrontal cortex. *The Journal of Neuroscience* 29(39):12315–12320.
- Churchland AK, Kiani R, Chaudhuri R, Wang XJ, Pouget A, Shadlen MN (2011) Variance as a Signature of Neural Computations during Decision Making. *Neuron* 69(4):818–831.
- Cisek P (2012) Making decisions through a distributed consensus. *Current Opinion in Neurobiology* 22(6):927–936.
- Cisek P, Kalaska JF (2010) Neural mechanisms for interacting with a world full of action choices. *Annual Review of Neuroscience* 33(1):269–298.
- Clithero JA, Rangel A (2013) Informatic parcellation of the network involved in the computation of subjective value. *Social cognitive and affective neuroscience* 9(9):1–14.
- Debreu G (1960) Individual Choice Behavior: A Theoretical Analysis by R. Duncan Luce. *The American Economic Review* 50(1):186–188.
- Ding L, Hikosaka O (2006) Comparison of Reward Modulation in the Frontal Eye Field and Caudate of the Macaque. *The Journal of Neuroscience* 26(25):6695–6703.
- Domenech P, Redouté J, Koechlin E, Dreher JC (2017) The Neuro-Computational Architecture of Value-Based Selection in the Human Brain. *Cerebral Cortex* 1–17.
- Dorris MC, Glimcher PW (2004) Activity in posterior parietal cortex is correlated with the relative subjective desirability of action. *Neuron* 44(2):365–378.

- Fehr E, Rangel A (2011) Neuroeconomic Foundations of Economic Choice—Recent Advances. *Journal of Economic Perspectives* 25(4):3–30.
- FitzGerald THB, Seymour B, Dolan RJ (2009) The role of human orbitofrontal cortex in value comparison for incommensurable objects. *The Journal of Neuroscience* 29(26):8388–8395.
- Ganguli D, Simoncelli EP (2014) Efficient Sensory Encoding and Bayesian Inference with Heterogeneous Neural Populations. *Neural Computation* 26(10):2103–2134.
- Glimcher PW (2005) Indeterminacy in Brain and Behavior. *Annual Review of Psychology* 56(1):25–56.
- Glimcher PW (2011) *Foundations of Neuroeconomic Analysis* (Oxford University Press).
- Gluth S, Spektor M, Rieskamp J (2016) Value-based attentional capture impairs trinary choice . *Society for Neuroeconomics Annual Meeting*.
- Gold JI, Shadlen MN (2007) The neural basis of decision making. *Annual Review of Neuroscience* 30:535–574.
- González-Vallejo C (2002) Making Trade-Offs: A Probabilistic and Context-Sensitive Model of Choice Behavior. *Psychological Review* 109(1):137–55.
- Greene WH (2003) *Econometric Analysis* (Prentice Hall), 5th edition.
- Hare TA, Malmaud J, Rangel A (2011a) Focusing attention on the health aspects of foods changes value signals in vmPFC and improves dietary choice. *The Journal of Neuroscience* 31(30):11077–11087.
- Hare TA, Schultz W, Camerer CF, O’Doherty JP, Rangel A (2011b) Transformation of stimulus value signals into motor commands during simple choice. *Proceedings of the National Academy of Sciences* 108(44):18120–18125.
- Hartline HK, Ratliff F (1957) Inhibitory interaction of receptor units in the eye of Limulus. *The Journal of general physiology* 40(3):357–376.
- Hawkins GE, Forstmann BU, Wagenmakers EJ, Ratcliff R, Brown SD (2015) Revisiting the Evidence for Collapsing Boundaries and Urgency Signals in Perceptual Decision-Making. *The Journal of Neuroscience* 35(6):2476–2484.
- Hebert B, Woodford M (2017) Rational Inattention with Sequential Information Sampling .
- Heeger DJ (1992) Normalization of cell responses in cat striate cortex. *Visual Neuroscience* 9(2):181–197.
- Holper L, Van Brussel LD, Schmidt L, Schulthess S, Burke CJ, Louie K, Seifritz E, Tobler PN (2017) Adaptive Value Normalization in the Prefrontal Cortex Is Reduced by Memory Load. *eNeuro* 4(2):1–20.
- Hsee CK, Loewenstein GF, Blount S, Bazerman MH (1999) Preference reversals between joint and separate evaluations of options: a review and theoretical analysis. *Psychological Bulletin* 125(5):576–590.
- Hubel DH, Wiesel TN (1968) Receptive fields and functional architecture of monkey striate cortex. *The Journal of Physiology* 195:215–243.
- Huber J, Payne JW, Puto C (1982) Adding Asymmetrically Dominated Alternatives: Violations of Regularity and the Similarity Hypothesis. *Journal of Consumer Research* 9(1):90–98.

- Hunt LT, Hayden BY (2017) A distributed, hierarchical and recurrent framework for reward-based choice. *Nature Reviews Neuroscience* 18(3):172–182.
- Ikeda T, Hikosaka O (2003) Reward-dependent gain and bias of visual responses in primate superior colliculus. *Neuron* 39(4):693–700.
- Izquierdo A (2004) Bilateral Orbital Prefrontal Cortex Lesions in Rhesus Monkeys Disrupt Choices Guided by Both Reward Value and Reward Contingency. *The Journal of Neuroscience* 24(34):7540–7548.
- Kahneman D, Tversky A (1979) Prospect Theory: An Analysis of Decision under Risk. *Econometrica: Journal of the Econometric Society* 47(2):263–292.
- Kennerley SW, Wallis JD (2009) Evaluating choices by single neurons in the frontal lobe: outcome value encoded across multiple decision variables. *European Journal of Neuroscience* 29(10):2061–2073.
- Klein JT, Deaner RO, Platt ML (2008) Neural Correlates of Social Target Value in Macaque Parietal Cortex. *Current Biology* 18(6):419–424.
- Klein TA, Ullsperger M, Jocham G (2017) Learning relative values in the striatum induces violations of normative decision making. *Nature Communications* 8:16033.
- Koszegi B, Rabin M (2006) A Model of Reference-Dependent Preferences. *Quarterly Journal of Economics* 121(4):1133–1165.
- Krajbich I, Armel C, Rangel A (2010) Visual fixations and the computation and comparison of value in simple choice. *Nature Neuroscience* 13(10):1292–1298.
- Landry P, Webb R (2019) Pairwise Normalization: A Neuroeconomic Theory of Multi-Attribute Choice. *SSRN Working Paper* .
- Levy D, Glimcher PW (2011) Comparing Apples and Oranges: Using Reward-Specific and Reward-General Subjective Value Representation in the Brain. *The Journal of Neuroscience* 31(41):14693–14707.
- Levy DJ, Glimcher PW (2012) The root of all value: a neural common currency for choice. *Current Opinion in Neurobiology* 22(6):1027–1038.
- Li V, Castañón SH, Solomon JA, Vandormael H, Summerfield C (2017) Robust averaging protects decisions from noise in neural computations. *PLoS Computational Biology* 13(8):e1005723.
- Lichtenstein S, Slovic P (2006) *The Construction of Preference* (Cambridge University Press).
- Lin A, Adolphs R, Rangel A (2012) Social and monetary reward learning engage overlapping neural substrates. *Social cognitive and affective neuroscience* 7(3):274–281.
- LoFaro T, Louie K, Webb R, Glimcher PW (2014) The Temporal Dynamics of Cortical Normalization Models of Decision-making . *Letters in Biomathematics* 1(2):209–220.
- Louie K, Glimcher PW (2010) Separating value from choice: delay discounting activity in the lateral intraparietal area. *The Journal of Neuroscience* 30(16):5498–5507.

- Louie K, Glimcher PW, Webb R (2015) Adaptive neural coding: from biological to behavioral decision-making. *Current Opinion in Behavioral Sciences* 5:91–99.
- Louie K, Grattan LE, Glimcher PW (2011) Reward value-based gain control: divisive normalization in parietal cortex. *The Journal of Neuroscience* 31(29):10627–10639.
- Louie K, Khaw MW, Glimcher PW (2013) Normalization is a general neural mechanism for context-dependent decision making. *Proceedings of the National Academy of Sciences* 110(15):6139–6144.
- Louie K, LoFaro T, Webb R, Glimcher PW (2014) Dynamic divisive normalization predicts time-varying value coding in decision-related circuits. *The Journal of Neuroscience* 34(48):16046–16057.
- Louviere J, Street D, Carson R, Ainslie A, DeShazo JR, Cameron T, Hensher D, Kohn R, Marley AAJ (2002) Dissecting the Random Component of Utility. *Marketing Letters* 13(3):177–193.
- Luce RD (1959) *Individual Choice Behaviour* (John Wiley and Sons, Inc.).
- Lyu S (2011) Dependency reduction with divisive normalization: justification and effectiveness. *Neural Computation* 23(11):2942–2973.
- Lyu S, Simoncelli EP (2008) Nonlinear image representation using divisive normalization. *2008 IEEE Conference on Computer Vision and Pattern Recognition (CVPR)*, 1–8 (IEEE).
- Machens CK, Gollisch T, Kolesnikova O, Herz A (2005) Testing the efficiency of sensory coding with optimal stimulus ensembles. *Neuron* 47:447–456.
- Mainen ZF, Sejnowski TJ (1995) Reliability of spike timing in neocortical neurons. *Science* 268(5216):1503–1506.
- Marley AAJ, Flynn TN, Louviere JJ (2008) Probabilistic models of set-dependent and attribute-level best–worst choice. *Journal of Mathematical Psychology* 52(5):281–296.
- McAdams CJ, Maunsell JHR (1999) Effects of Attention on Orientation-Tuning Functions of Single Neurons in Macaque Cortical Area V4. *The Journal of Neuroscience* 19(1):431–441.
- McFadden DL (2001) Economic choices. *The American Economic Review* 91(3):351–378.
- McNamee D, Rangel A, O’Doherty JP (2013) Category-dependent and category-independent goal-value codes in human ventromedial prefrontal cortex. *Nature Neuroscience* 16(4):479–485.
- Meyer RJ (1991) Probabilistic Models of Consumer Choice Behavior. Robertson TS, ed., *Handbook of Consumer Behavior* (Prentice Hall, Inc.).
- Moisa M, Polania R, Grueschow M, Lee YJ, Nagy Z, Ruff C (2018) A causal account of the brain network mechanisms underlying value-based choices. *Society for Neuroeconomics Annual Meeting*.
- Netzer N (2009) Evolution of Time Preferences and Attitudes toward Risk. *The American Economic Review* 99(3):937–955.
- Noguchi T, Stewart N (2018) Multialternative Decision by Sampling: A Model of Decision Making Constrained by Process Data. *Psychological Review* 125(4):512–544.

- Noonan MP, Chau B, Rushworth MF, Fellows LK (2017) Contrasting effects of medial and lateral orbitofrontal cortex lesions on credit assignment and decision making in humans. *The Journal of Neuroscience* 37(29):0692–17–7035.
- Ongür D, Price JL (2000) The organization of networks within the orbital and medial prefrontal cortex of rats, monkeys and humans. *Cerebral Cortex* 10(3):206–219.
- Padoa-Schioppa C (2009) Range-adapting representation of economic value in the orbitofrontal cortex. *The Journal of Neuroscience* 29(44):14004–14014.
- Padoa-Schioppa C (2011) Neurobiology of Economic Choice: A Good-Based Model. *Annual Review of Neuroscience* 34(1):333–359.
- Padoa-Schioppa C, Assad JA (2006) Neurons in the orbitofrontal cortex encode economic value. *Nature* 441(7090):223–226.
- Padoa-Schioppa C, Conen KE (2017) Orbitofrontal Cortex: A Neural Circuit for Economic Decisions. *Neuron* 96(4):736–754.
- Pastor-Bernier A, Cisek P (2011) Neural correlates of biased competition in premotor cortex. *The Journal of Neuroscience* 31(19):7083–7088.
- Plassmann H, O’Doherty JP, Rangel A (2007) Orbitofrontal cortex encodes willingness to pay in everyday economic transactions. *The Journal of Neuroscience* 27(37):9984–9988.
- Platt ML, Glimcher PW (1999) Neural correlates of decision variables in parietal cortex. *Nature* 400:233–238.
- Platt ML, Plassmann H (2013) Multistage Valuation Signals and Common Neural Currencies. *Neuroeconomics* (Academic Press).
- Polania R, Moisa M, Opitz A, Grueschow M, Ruff CC (2015) The precision of value-based choices depends causally on fronto-parietal phase coupling. *Nature Communications* 6(1):8090.
- Polania R, Woodford M, Ruff CC (2019) Efficient coding of subjective value. *Nature Neuroscience* 22(1):134–142.
- Porrino LJ, Crane AM, Rakic PSG (1981) Direct and indirect pathways from the amygdala to the frontal lobe in rhesus monkeys. *Journal of Comparative Neurology* 198(1):121–136.
- Qamar AT, Cotton RJ, George RG, Beck JM, Prezhdo E, Laudano A, Tolia AS, Ma WJ (2013) Trial-to-trial, uncertainty-based adjustment of decision boundaries in visual categorization. *Proceedings of the National Academy of Sciences* 110(50):20332–20337.
- Rangel A, Clithero JA (2012) Value normalization in decision making: theory and evidence. *Current Opinion in Neurobiology* 22(6):970–981.
- Ratcliff R (1978) A theory of memory retrieval. *Psychological Review* 85(2):59–108.
- Rayo L, Becker GS (2007) Evolutionary Efficiency and Happiness. *Journal of Political Economy* 115(2):302–337.

- Rich EL, Wallis JD (2016) Decoding subjective decisions from orbitofrontal cortex. *Nature Neuroscience* 19(7):973–980.
- Rieskamp J, Busemeyer JR, Mellers B (2006) Extending the bounds of rationality: evidence and theories of preferential choice. *Journal of Economic Literature* 44(3):631–661.
- Robson AJ (2001a) The biological basis of economic behavior. *Journal of Economic Literature* 39(1):11–33.
- Robson AJ (2001b) Why would nature give individuals utility functions? *Journal of Political Economy* 109(4):900–914.
- Robson AJ, Samuelson L (2010) The Evolutionary Foundations of Preferences. Benhabib J, Bisin A, Jackson M, eds., *Handbook of Social Economics*, 221–310 (North Holland).
- Roitman JD, Shadlen MN (2002) Response of Neurons in the Lateral Intraparietal Area during a Combined Visual Discrimination Reaction Time Task. *The Journal of Neuroscience* 22(21):9475–9489.
- Rorie AE, Gao J, McClelland JL, Newsome WT (2010) Integration of sensory and reward information during perceptual decision-making in lateral intraparietal cortex (LIP) of the macaque monkey. *PloS one* 5(2):e9308.
- Rudebeck PH, Saunders RC, Lundgren DA, Murray EA (2017) Specialized representations of value in the orbital and ventrolateral prefrontal cortex: desirability versus availability of outcomes. *Neuron* 95:1208–1220.
- Rust NC, Mante V, Simoncelli EP, Movshon JA (2006) How MT cells analyze the motion of visual patterns. *Nature Neuroscience* 9(11):1421–1431.
- Salisbury LC, Feinberg F (2010) Alleviating the constant stochastic variance assumption in decision research: Theory, measurement, and experimental test. *Marketing Science* 29(1):1–17.
- Samejima K (2005) Representation of action-specific reward values in the striatum. *Science* 310(25):1337–1340.
- Samuelson PA (1948) *Foundations of Economic Analysis*.
- Schwartz O, Simoncelli EP (2001) Natural signal statistics and sensory gain control. *Nature Neuroscience* 4(8):819–825.
- Seymour B, McClure SM (2008) Anchors, scales and the relative coding of value in the brain. *Current Opinion in Neurobiology* 18(2):173–178.
- Shadlen MN, Kiani R (2013) Decision making as a window on cognition. *Neuron* 80(3):791–806.
- Shadlen MN, Newsome WT (1998) The variable discharge of cortical neurons: implications for connectivity, computation, and information coding. *The Journal of Neuroscience* 18(10):3870–3896.
- Shadlen MN, Newsome WT (2001) Neural Basis of a Perceptual Decision in the Parietal Cortex (Area LIP) of the Rhesus Monkey. *Journal of Neurophysiology* 86(4):1916–1936.

- Shadlen MN, Shohamy D (2016) Decision making and sequential sampling from memory. *Neuron* .
- Shannon CE (1948) A Mathematical Theory of Communication. *Bell System Technical Journal* 27(3):379–423.
- Simon HA (1979) Rational Decision Making in Business Organizations. *The American Economic Review* 69(4):493–513.
- Simonson I (1989) Choice Based on Reasons: The Case of Attraction and Compromise Effects. *Journal of Consumer Research* 16(2):158–174.
- Sims CA (2003) Implications of rational inattention. *Journal of Monetary Economics* 50(3):665–690.
- Sinz F, Bethge M (2013) Temporal Adaptation Enhances Efficient Contrast Gain Control on Natural Images. *PLoS Computational Biology* 9(1):e1002889.
- Slovic P, Lichtenstein S (1983) Preference Reversals: A Broader Perspective. *The American Economic Review* 73(4):596–605.
- Smith A, Bernheim BD, Camerer CF, Rangel A (2014) Neural Activity Reveals Preferences without Choices. *American Economic Journal: Microeconomics* 6(2):1–36.
- Soltani A, De Martino B, Camerer CF (2012) A range-normalization model of context-dependent choice: a new model and evidence. *PLoS Computational Biology* 8(7):e1002607.
- Steiner J, Stewart C (2016) Perceiving prospects properly. *The American Economic Review* .
- Stevens CF (2003) Neurotransmitter release at central synapses. *Neuron* 40(2):381–388.
- Stevens SS (1961) To Honor Fechner and Repeal His Law: A power function, not a log function, describes the operating characteristic of a sensory system. *Science* 133(3446):80–86.
- Steverson K, Brandenburger A, Glimcher PW (2018) Choice-Theoretic Foundations of the Divisive Normalization Model. *SSRN Working Paper* .
- Sugrue LP, Corrado GS, Newsome WT (2004) Matching Behavior and the Representation of Value in the Parietal Cortex. *Science* 304:1782–1787.
- Summerfield C, Tsetsos K (2012) Building Bridges between Perceptual and Economic Decision-Making: Neural and Computational Mechanisms. *Frontiers in Neuroscience* 6.
- Suzuki S, Cross L, O’Doherty JP (2017) Elucidating the underlying components of food valuation in the human orbitofrontal cortex. *Nature Neuroscience* 20(12):1780–1786.
- Swait J, Marley AAJ (2013) Probabilistic choice (models) as a result of balancing multiple goals. *Journal of Mathematical Psychology* 57(1-2):1–14.
- Tolhurst DJ, Movshon JA, Dean AF (1983) The statistical reliability of signals in single neurons in cat and monkey visual cortex. *Vision research* 23(8):775–785.
- Train KE (2009) *Discrete Choice Methods with Simulation* (Cambridge University Press), 2nd edition.

- Tremblay L, Schultz W (1999) Relative reward preference in primate orbitofrontal cortex. *Nature* 398(6729):704–708.
- Trueblood JS, Brown SD, Heathcote A (2014) The multiattribute linear ballistic accumulator model of context effects in multialternative choice. *Psychological Review* 121(2):179–205.
- Tsetsos K, Usher M, Chater N (2010) Preference reversal in multiattribute choice. *Psychological Review* 117(4):1275–1293.
- Tversky A (1972) Elimination by aspects: A theory of choice. *Psychological Review* 79(4):281–299.
- Tymula AA, Glimcher PW (2016) Expected Subjective Value Theory (ESVT): A Representation of Decision Under Risk and Certainty. *SSRN Working Paper* .
- Tymula AA, Woelbert E, Glimcher PW (2016) Flexible Valuations for Consumer Goods as Measured by the Becker–DeGroot–Marschak Mechanism . *Journal of Neuroscience, Psychology, and Economics* 9(2).
- Vuong QH (1989) Likelihood Ratio Tests for Model Selection and Non-Nested Hypotheses. *Econometrica: Journal of the Econometric Society* 57(2):307.
- Wainwright MJ, Schwartz O, Simoncelli EP (2001) Natural Image Statistics and Divisive Normalization: Modeling Nonlinearities and Adaptation in Cortical Neurons. *Statistical Theories of the Brain* (MIT Press).
- Wang AY, Miura K, Uchida N (2013) The dorsomedial striatum encodes net expected return, critical for energizing performance vigor. *Nature Neuroscience* 16(5):639–647.
- Wasserman L (2000) Bayesian Model Selection and Model Averaging. *Journal of Mathematical Psychology* 44(1):92–107.
- Webb R (2019) The (Neural) Dynamics of Stochastic Choice. *Management Science* 65(1):230–255.
- Webb R, Levy I, Lazzaro S, Rutledge RB, Glimcher PW (2019) Neural Random Utility: Relating Cardinal Neural Observables to Stochastic Choice Behaviour. *Journal of Neuroscience, Psychology, and Economics* 12(1):45–72.
- Weber E (1834) *On the Tactile Senses (with translation of De Tactu)* (Experimental Psychology Society, New York).
- Weber EU, Johnson EJ (2009) Mindful Judgment and Decision Making. *Annual Review of Psychology* 60(1):53–85.
- Wei XX, Stocker AA (2017) Lawful relation between perceptual bias and discriminability. *Proceedings of the National Academy of Sciences* 114(38):10244–10249.
- Wilcox NT (2011) ‘Stochastically more risk averse:’ A contextual theory of stochastic discrete choice under risk. *Journal of Econometrics* 162(1):89–104.
- Woodford M (2012) Prospect Theory as Efficient Perceptual Distortion. *The American Economic Review* 102(3):41–46.

Yoo SBM, Hayden BY (2018) Economic Choice as an Untangling of Options into Actions. *Neuron* 99(3):434–447.

Zimmermann J, Glimcher PW, Louie K (2018) Multiple timescales of normalized value coding underlie adaptive choice behavior. *Nature Communications* 9(1):3206.